R-5

Critical Reviews in Biomedical Engineering, 19(4):293–340 (1992)

Electrically Evoked Myoelectric Signals

Roberto Merletti, Ph.D. and Marco Knaflitz, Ph.D.*
NeuroMuscular Research Center, Department of Biomedical Engineering, Boston University, Boston, MA; and Department of Electronics, Politecnico di Torino, Torino, Italy

Carlo J. DeLuca, Ph.D.
NeuroMuscular Research Center, Department of Biomedical Engineering, Boston University, Boston, MA

* Address all correspondence to Dr. Roberto Merletti, NeuroMuscular Research Center, 44 Cummington Street, Boston, MA 02215

ABSTRACT: Electrical stimulation of the nervous system is attracting increasing attention because of the possibilities it offers for physiological investigations, clinical diagnosis, muscle function assessment, noninvasive muscle characterization, and functional control of paralyzed extremities.

Parameters of the myoelectric signal evoked by surface stimulation of a muscle motor point or by stimulation of a nerve trunk by means of implanted electrodes provide information about muscle performance and properties if the stimulation artifact is properly removed or suppressed. Comparison of these parameters with those obtained during voluntary contractions provides additional insight into muscle physiology. The relationships between myoelectric signal amplitude parameters, spectral parameters, and conduction velocity are discussed with special reference to muscle fatigue.

This review focuses on a few methodological aspects concerning electrical stimulation of the peripheral nervous system, detection, and processing of the electrically evoked myoelectric signals in skeletal muscles. The state of the art of the following issues is discussed: (1) properties of voluntary and electrically evoked myoelectric signals; (2) techniques for evoking and detecting myoelectric signals; (3) techniques for suppression of stimulation artifacts; (4) effect of stimulation waveforms and electrode properties; (5) signal processing techniques for electrically evoked myoelectric signals; (6) physiological significance of myoelectric signal variables; (7) order of recruitment of motor units during electrical stimulation; (8) myoelectric manifestations of fatigue in electrically stimulated muscles; (9) assessment of crosstalk by electrical stimulation; and (10) applications in sport, rehabilitation, and geriatric medicine.

KEY WORDS: crosstalk, electrical stimulation, electromyography, human muscles, muscle fatigue, M-wave, myoelectric signal.

ACRONYMS AND ABBREVIATIONS

ARV = Average rectified value
CNS = Central nervous system
CV = Conduction velocity of muscle fibers
DD = Double differential
FES = Functional electrical stimulation
MDF = Median frequency of the myoelectric signal power spectral density function
MNF = Mean frequency of the myoelectric signal power spectral density function
MUAP = Motor unit action potential
MVC = Maximal voluntary contraction
M-wave = Myoelectric signal evoked in response to each electrical stimulus
RMS = Root mean square value
PSD = Power spectral density function (or power spectrum) of a signal
SD = Single differential

0278-940X/92/$.50

I. INTRODUCTION

Electrical stimulation of the neuromuscular system is used in a variety of research, diagnostic, therapeutic, and orthotic applications. In research applications, electrical stimulation is used to investigate the physiological properties of the neuromuscular system. The technique is also useful in investigating whether muscle fatigue is due to the failure of neuromuscular transmission, to factors related to muscle fiber membrane excitability, or to intracellular phenomena. In diagnostic applications, it is used to ascertain the integrity of neuromuscular junctions and reflex loops, as well as the excitability of motoneuron pools, nerves, and muscle fibers. All these applications require the detection of the electrical response of the muscle fibers to an electrical stimulus applied under controlled conditions to the motoneurons, their terminal branches, or directly to the muscle fibers. In therapeutic applications, it is used to maintain muscle mass, muscle function, and enhance blood flow during immobilization periods or following lesions of the peripheral (PNS) or central nervous system (CNS). Electrical stimulation is extensively used in clinical practice to prevent disuse or denervation atrophy, to reduce spasticity, and to improve voluntary control in stroke patients. Most recently, it has found applications in space medicine for counteracting the effect of microgravity on muscle and bone tissue.[46] In orthotic applications, electrical stimulation is used to provide external control of paralyzed muscles for functional purposes. This application is commonly referred to as functional electrical stimulation (FES).[88] The recent development of cardiac assistive devices that employ transplanted skeletal muscles has shown promise.[10,99] The spectrum of research and clinical applications of neuromuscular stimulation is clearly wide-ranging. This review does not attempt to cover the complete theater of activity; instead, it focuses on a few methodological aspects concerning electrical stimulation of the PNS, as well as the detection and processing techniques that apply to the electrically evoked myoelectric signals in skeletal muscles. The following issues are *not* dealt with in this review: (1) motor cortex or spinal cord stimulation, (2) reflex studies and studies of denervated muscles, and (3) studies of sphincter, smooth, and cardiac muscles. The issues addressed in this work are

1. Properties of voluntary and electrically evoked myoelectric signals
2. Evoking and detecting myoelectric signals
3. Suppression of the stimulation artifact
4. Effect of stimulation waveform and electrode properties
5. Parameters and processing techniques for electrically evoked myoelectric signals
6. Physiological significance of myoelectric signal variables
7. Order of recruitment of motor units during electrical stimulation
8. Myoelectric manifestation of fatigue in electrically stimulated muscle
9. Assessment of crosstalk by electrical stimulation
10. Possible applications in sport, rehabilitation, and geriatric medicine

II. VOLUNTARY VS. ELECTRICALLY EVOKED MYOELECTRIC SIGNALS

A skeletal muscle consists of a number of motor units, which in turn consist of a number of muscle fibers innervated by the terminal branches of a single α-motoneuron whose cell body is located in the anterior horn of the spinal cord. The CNS and PNS control muscle performance by modulating the number of recruited motoneurons and the firing rate of the motoneurons. These two factors are determined by the synaptic activity on the cell body of each motoneuron, and this is a function of the activity of the descending upper motoneurons and of the afferent activity emanating from a number of peripheral sensors. The individual terminal branch of a motoneuron innervates a muscle fiber at an intermediate point. Each firing of the motoneuron triggers, through the neuromuscular junction, a depolarization that propagates in opposite directions toward the two ends of the muscle fiber. This action generates two action potentials traveling at a speed referred to as the muscle fiber conduction velocity (CV). The action potential of muscle fibers belonging to the same motor unit is not precisely synchronized in either space or time because of different lengths of motoneuron terminal branches, spatial scattering of the neuromuscular junctions, and possible fiber to fiber variations of the CV. The sum of these single fiber contributions is referred to as the motor unit action potential (MUAP) and the sequence of these MUAPs is known as the MUAP train.

The firing sequence of the MUAPs is described by the firing rate which is calculated from the inverse of the firing interval. The firing rates of different motor units within a muscle and across muscles are controlled in a tightly bound manner and are significantly cross-correlated with a near-zero phase shift. The unison behavior of the firing rates is called the **common drive**. This phenomenon indicates that the nervous system controls the motor units in a nonindividual fashion.

Each active MUAP has an associated current field in the surrounding volume conductor. This field is comprised of the nonlinear sum of the electrical fields generated by the individual muscle fibers of the motor unit. Two electrodes may be used to detect the potential difference between any two points inside or on the boundaries of the volume conductor. The potential detected by this electrode pair is the weighted sum of the contributions of the different generators. The weight of each component is determined by the distance of the corresponding source from the detection electrode pair and the anisotropy of the tissue. The detection electrode pair itself introduces an additional filtering function related to the inter-electrode distance[97] (see Section III). For a more detailed description of the myoelectric signal generation process and for details about units, terms, and standards in reporting electromyography research, the reader is referred to the first three chapters of the book *Muscles Alive*,[14] to the original work of Lindstrom and Magnusson,[97] and to the Report of the Ad Hoc Committee of the International Society of Electrophysiological Kinesiology.

During voluntary contractions, MUAPs are almost asynchronous and the resulting potential difference between the detection electrodes is stochastic, with a probability density function that is approximately Gaussian if a sufficiently large number of active motor units contribute to the electrode potential. During electrical stimulation of either the terminal branches or the axons of the motoneurons, the MUAPs are evoked and synchronized by the external stimuli, therefore generating an evoked response referred to as the compound action potential (CAP), or M-wave, associated with each stimulus. This response is a *quasi-deterministic* signal since differences between adjacent responses are minor.

In addition to the orthodromic volley of nerve action potentials, electrical stimulation produces an antidromic volley, as well as a volley along afferent sensory fibers, which may occasionally cause F or H reflexes. Hence, in the absence of simultaneous voluntary activation, the electrically evoked myoelectric signal is a function of the stimulation modalities, the properties of the muscle, and the geometry of the detection electrode system. The evoked response is entirely controlled by external conditions. Figure 1A and B provide a schematic description of the mechanism leading to voluntary and electrically evoked myoelectric signals, which are entirely different modalities of muscle activation. The myoelectric signals evoked by the two modalities may therefore provide different, and possibly complementary, information on muscle structure and behavior. Electrical stimulation of α-motoneurones provides ways to test the muscle "motor" isolated from CNS control, under open loop conditions, with a wide range of experimental options and a higher degree of control of the experimental paradigms.

III. EVOKING AND DETECTING MYOELECTRIC SIGNALS

The overall system for the investigation of electrically evoked myoelectric signals consists of stimulation and detection units. They may be independent and separated or may be closely associated in a single instrument. Stimulation artifact removal is a major issue when surface stimulation and detection techniques are used. This issue is particularly relevant if the stimulation and detection electrodes are relatively close and is addressed in Section IV.

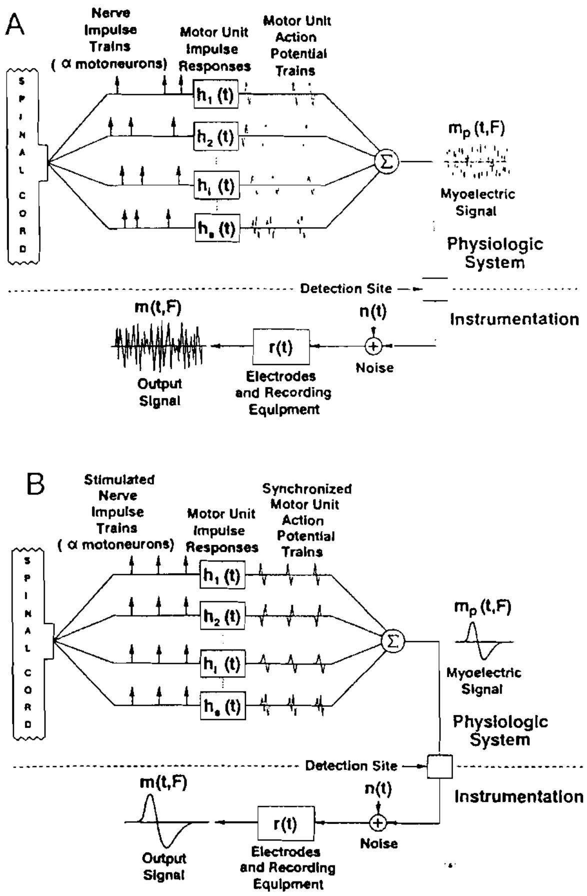

FIGURE 1. (A) Model of the surface myoelectric signal generation mechanism during voluntary contractions. The signal is the sum of contributions from asynchronously firing motor units, and is stochastic with near-Gaussian amplitude distribution. (B) Model of the surface myoelectric signal generation mechanism during electrically evoked contractions. The signal is the sum of contributions from synchronously firing motor units, it is quasideterministic and periodic, with a repetition rate equal to the stimulation rate.

A. Stimulation Techniques

Myoelectric signals (M-waves) may be evoked in several ways: (1) by electrically stimulating the CNS; (2) by stimulating the peripheral nerves with implanted cuffs, neural electrodes, or surface electrodes; (3) by stimulating the terminal axonal branches with wire electrodes implanted in the muscle, with subcutaneous electrodes placed on the surface of the muscle, or with surface electrodes placed on the skin above a motor point; and (4) by direct stimulation of the muscle fibers. This review focuses solely on techniques (2) and (3), with particular attention to surface methods.

Since current flow from the stimulation to the detection electrodes or from the stimulation electrodes to mains ground (system ground) is highly undesirable for reasons related to subject safety as well as to signal quality, the output stage of the stimulator must be isolated from ground and from any other circuit or instrument. This isolation is usually achieved by means of optical or electromagnetic couplers (optical isolators, transformers). Two stimulation techniques are commonly used:

1. *Monopolar technique:* the term ''monopolar'' refers to the fact that the electrical stimulation occurs in the vicinity of only one of the two electrodes and not at the other. The stimulation electrode is located near a nerve or on or near a muscle motor point and the second electrode is located on a bony prominence or away from excitable tissue. The same advantage may be obtained by using a second electrode with a surface sufficiently large to assure that the current density in its vicinity is below the excitation threshold. Although suprathreshold current density levels may be achieved only underneath the stimulating electrode, the current field obtained via this technique occupies a large region of space. If this region includes the detection electrodes, artifact problems will arise (refer to Section IV for details).
2. *Bipolar technique:* two electrodes (usually of similar size) are applied on or near the tissue to be electrically activated. With respect to the monopolar technique, stimulation is less localized since it may take place under either or both electrodes. The advantage of this approach, however, is that the current distribution is more confined in space. If the distance between detection and stimulation electrodes is at least an order of magnitude greater than the stimulation interelectrode distance, artifact problems may be less relevant that with the monopolar technique.

Two basic types of stimulator output stage exist:

1. *Voltage-controlled output stages:* in this case the output impedance of the stimulator is at least an order of magnitude lower than that of the interelectrode impedance. Thus, the interelectrode voltage is maintained reasonably constant despite variations in the interelectrode impedance. Such variations may modify unpredictably the stimulation current and, therefore, evoke varying responses from the muscle. Between stimuli, these stages behave as an active short circuit, thus providing a low-impedance path for discharging electrode and tissue capacitances. As a consequence, part of the stimulation artifact may be effectively reduced[82,108] (refer to Section IV for details).
2. *Current-controlled output stages:* in this case, the output impedance is at least an order of magnitude higher than the interelectrode impedance. This case generally provides more controllable responses to stimulation. Between stimuli, this output stage behaves as an open circuit; therefore, electrode and tissue capacitances find a relatively high impedance discharge path through the tissues and the resistive component of the metal-electrolyte interface, and this yields slowly decaying voltage transients across the stimulating electrodes.[82,108]

The applied stimulus may be either mono- or biphasic, the latter having the advantage of reversing the polarity of the output voltage or current so that a near-zero charge shift occurs across the electrodes and the excited tissue; it usually has no DC component. Since the tissues are not purely resistive and linear, the shape of the voltage and current waveforms is not necessarily the same. Another factor to consider when electrically stimulating a muscle is the amount of muscle tissue that is activated. It has been reported[17,81] that, when a motor nerve is stimulated directly and supramaximally, the joint torque approaches 100% of the maximal force evoked by voluntary contraction (MVC), suggesting that a comparable portion of the muscle (possibly the entire muscle) is activated by the two methods. On the other hand, electrical activation of the terminal branches of the motor axons, obtained by monopolar stimulation of a motor point, results in comparatively less discomfort for the subject, but produces activation of only the most superficial nerve branches. Although higher selectivity is achieved, full activation of a single muscle is not easily obtained and the maximal evoked force is usually below 40% MVC.[120]

B. Signal Detection and Conditioning Techniques

Detection techniques for electrically evoked myoelectric signals are not substantially different from those used for detecting voluntarily evoked signals. Surface electrodes are typically used for this purpose. If both electrodes are within or above the muscle, the detection is said to be bipolar. If only one electrode is within or above the muscle and the other is on an electrically inactive region, the detection is said to be monopolar. The characteristics of both passive and active surface electrodes have been described extensively elsewhere (see Reference 14, among others). When using surface electrodes it is important to realize that the surface myoelectric signal (and the M-wave, in particular) may be described as a space distribution of an electric potential that is traveling along the direction of the muscle fibers from the innervation zone to the end of the fibers with CV $= v$. The space and time description of the signal are related by the following basic equations which hold for a periodic signal or for each frequency component of a nonperiodic signal:

$$v = \lambda f_t = \lambda / T; \quad f_s = 1/\lambda = f_t / v \qquad (1)$$

where: v = conduction velocity (CV), [m/s]; λ = wavelength, [m]; f_t = frequency in the time domain, [cycles/s or Hz]; T = period, [s]; and f_s = frequency in the space domain, [cycles/m].

The differential technique indicated in Figure 2A is the standard method for detecting the myoelectric signal. At any given time, the differential amplifier receives two space samples of the signal from the two detection surfaces separated by the interelectrode distance d, and computes their difference. If distances are measured with respect

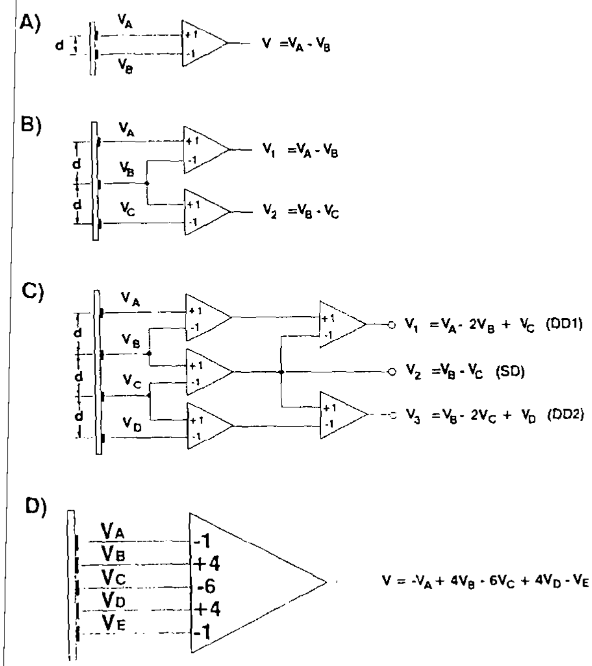

FIGURE 2. Surface myoelectric signal detection systems.[25,139,140] (A) Single differential detection system, (B) dual single differential detection system, (C) double differential detection system, and (D) quadruple differential detection system.

to the middle of the interelectrode spacing, the output may be described as sampled in space by $\delta(-d/2) - \delta(d/2)$ where δ is the Dirac function. The Fourier transform of the output signal (in the f_t domain), $F(2\pi f)$, is

$$
\begin{aligned}
F(2\pi f_t) &= F_m(2\pi f_t)(e^{-j2\pi f_t d/2v} \\
&\quad - e^{j2\pi f_t d/2v}) \\
&= -2j \sin \pi f_t d/v F_m(2\pi f_t) \\
&= H(2\pi f_t) F_m(2\pi f_t) \qquad (2)
\end{aligned}
$$

where: $F_m(2\pi f_t)$ = Fourier transform of the monopolar signal; $H(2\pi f_t)$ = transfer function of the two-electrode system; and f_t = frequency in the time domain, [cycles/s or Hz].

For d that is much smaller than the smallest λ of interest, the differential detection system behaves like a differentiating filter with a slope of 6 dB per octave and a gain of d/v. It is therefore clear that the interelectrode distance and CV affect the waveform of the detected signal.[97] Such a difference is not clearly evident during voluntary contractions because of the stochastic nature of the signals. The phenomenon is more obvious when electrically evoked signals are analyzed. Greater interelectrode distances invariably bring the two detection surfaces closer to the innervation zones and to the end of the fibers. At these two locations, the shape of the signal is altered by the superposition effect of bidirectionally traveling signals and the abrupt termination of signal propagation.

When using surface electrodes, it is important to consider the CV of the myoelectric signal because, as was shown above, it affects the information content of the signal. The three-detection bars-single-differential (SD) detection system presented in Figure 2B is theoretically sufficient to measure the CV if only traveling signals are present. Such is not the case in general, however, and standing or near-standing myoelectric signals may be present on the surface of the skin. To deal with this complication, Broman et al.[25] proposed an electrode consisting of four equally spaced detection bars connected to a double differential (DD) amplifier, as reported in Figure 2C. The impulse response and the transfer function of this system (in the space, time, spatial-frequency, and time-frequency domains, respectively) for either of the two DD outputs V_1 or V_2 and for $x = 0$ centered under the middle bar of each three-bar detection system is given by:

$$
\begin{aligned}
h(x) &= \delta(x - d) - 2\delta(x) + \delta(x + d); \\
h(t) &= \delta(t - d/v) - 2\delta(t) + \delta(t + d/v)
\end{aligned}
\qquad (3)
$$

$$
\begin{aligned}
H(2\pi f_s) &= 2(\cos 2\pi d/\lambda - 1); \\
H(2\pi f_t) &= 2(\cos 2\pi\, df_t/v - 1)
\end{aligned}
\qquad (4)
$$

where x represents the space domain and t represents the time domain.

It is interesting and important to observe that both domains present a zero transmission for any integer value of the ratio $d/\lambda = df_t/v$. This null, reflected in the spectrum of either the SD or DD signals, is referred to as a *spectral dip*.[97] The second layer of differential amplifiers provides two DD outputs V_1 and V_2, which do not contain any contribution from SD input signals common to all sequential pairs of electrodes. The time delay between the two outputs V_1 (DD1) and V_2 (DD2) is given by d/v and is theoretically not affected by common stationary SD signals of equal amplitudes, therefore providing a better estimate of the delay than the circuit of Figure 2B.[25] From a technical point of view, this arrangement may be described as a spatial finite impulse response filter with zero phase rotation.[132] In practice, the four-bar electrode yields three signals consisting of an SD output from which amplitude and spectral variables may be computed, and two DD outputs (DD1 and DD2) from which CV may be computed. It is possible to demonstrate that the spatial resolution of the SD output is lower than that of DD outputs, an important feature for the detection of crosstalk (see Section X), and that the DD (or higher order; Figure 2D) systems behave as "near pass" filters.[139,140]

Regardless of which technique is used to detect the myoelectric signal, it is necessary to appreciate the mechanical difficulties in detecting stable responses to an individual stimulus or short bursts of excitation. Under these circumstances, even as concerns isometric conditions of the joint, considerable movement of the muscle tissue may occur with respect to the detection electrode, transients in the CV, and possible movement between the stimulation electrode and the nerve fibers. All these factors would produce variability in the shape of the detected M-wave. An example of the observed variability is presented in Figure 3. This case demonstrates the variability associated with consecutive firings at the beginning of a stimuli train before the muscle reaches tetanus.

Indwelling wire electrodes have been used by Lam et al.[93] to detect myoelectric signals evoked in the gastrocnemius of the cat by electrical stimulation of the sciatic nerve. These authors found that the average rectified value of electrically evoked signals detected from different muscle sites shows considerable variation and suggested that only the summation of signals from different electrode pairs may provide an unbiased

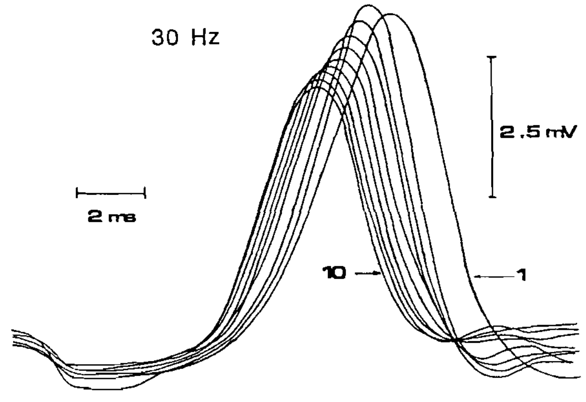

FIGURE 3. An example of the transient behavior of the M-wave at the beginning of an electrically evoked isometric contraction of the human tibialis anterior muscle; supramaximal stimulation of the main muscle motor point at 30 Hz. The first ten responses are displayed.

description of the activity of the muscle. Unfortunately, Lam and co-authors provided no indication of the variability of the M-wave shape from different electrode pairs.

A major difference in signal conditioning between voluntary and electrically evoked surface myoelectric signals is the need to remove the stimulation artifact. This issue is discussed in detail in the next section. An example of a complete stimulation/detection system used in recent research[82,85,112,114] is reported in Figure 4.

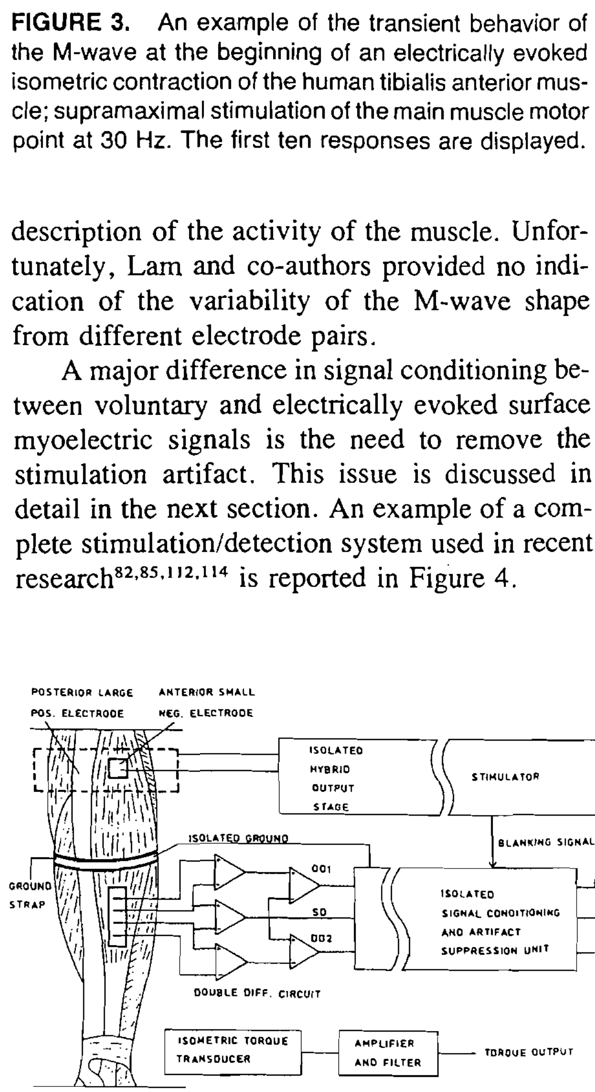

FIGURE 4. Complete stimulation/detection system with artifact suppression features.[82,112] See Figures 6, 7, and 8 for greater details.

IV. SUPPRESSION OF THE STIMULATION ARTIFACT FROM THE MYOELECTRIC SIGNAL

A common problem encountered in the analysis of electrically evoked biopotentials is the presence of the stimulation artifact. If stimulation is administered by means of invasive electrodes, such as wires, needles, or nerve cuffs, the current field is usually limited to a relatively small tissue volume and does not extend to the detection volume of the myoelectric signal detection electrode unless high current levels are used.[14,147,149]

The situation becomes much more critical when surface stimulation electrodes and surface detection electrodes are used. In the latter case, the current field extends to a large volume of tissue that usually includes the detection volume of the detection electrode. Myoelectric signals (M-waves) obtained by stimulating a muscle motor point and detected on the same muscle may be contaminated by artifacts whose amplitude is from one to two orders of magnitude greater than the M-waves. These artifacts may cause saturation of the front end of the myoelectric signal amplifier, but even when the saturation level is not reached, M-waves may be detrimentally affected by artifacts.

According to the scheme suggested by McGill et al.,[108] the analysis of the stimulation artifact must include the following points:

1. Characterization of the skin-electrode interface, for both detection and stimulation electrodes
2. Electrical characterization of the subcutaneous tissue
3. Design of the output stage of the neuromuscular stimulator
4. Design of the myoelectric signal amplifier

A. Skin-Electrode Interface

Electric phenomena taking place at the skin-electrode interface are complex and not completely understood.[49,60,108,154] The major difference between detection and stimulation electrodes is the amount of current density at the electrode-skin interface. Current density ranges between 1 and 100 mA/cm^2 underneath stimulation electrodes, while it is several orders of magnitude lower underneath detection electrodes. For both detection and stimulation electrodes, the two major components of the interface are the metal-electrolyte junction and the skin. Both components are nonlinear. The metal-electrolyte junction has been widely studied and modeled by a number of researchers (see References 60 and 154, among others) as a double-charge layer that produces the DC half-cell potential, a polarization capacitance that depends on frequency and current density, and a relatively large electrolytic capacitance. The outer layers of the skin (keratinous layer and epidermis) behave like a resistive sheath around a volume conductor.[47,60,108,157] The resistance of this sheath is known to decrease with increasing current density and is affected by cleaning and abrasion and by the activity of sweat glands. In summary:

1. In detection electrodes, at very low current densities, the electrode-skin interface may be modeled by a parallel RC cell,[60,61,108] with both R and C fixed and mainly dependent upon electrode geometry. The half-cell DC potential and the galvanic skin potential may be neglected in most practical cases since they are generally blocked by high-pass filter of the recording amplifier.
2. In stimulation electrodes, at high current densities, the electrode-skin interface may be described adequately by a simple model proposed by Stephens.[154] The model consists of a nonlinear resistor featuring a parabolic V-I relationship ($I = \alpha V + \beta V^2$) in parallel with a fixed capacitance.

B. Subcutaneous Tissue

Subcutaneous tissue is neither homogeneous nor isotropic, but is generally conveniently modeled as a purely resistive volume conductor,[60,108,134,157] an approximation that is considered acceptable for studying artifact suppression. The resistance of subcutaneous tissue between two different points in the same limb generally ranges between 100 and 500 Ω.[108] Most of the stimulus voltage drops across the impedances of the stimulating electrodes and the skin, and consequently potentials induced within the limb are generally a small fraction of those produced by the stimulator output stage.

C. Output Stage of Neuromuscular Stimulators

As discussed in Section III, the output stage of a neuromuscular stimulator may be a voltage- or a current-controlled stage. Current-controlled stages provide a current that is virtually insensitive to variations of the interelectrode impedances but leads to long stimulus artifacts. On the other hand, voltage-controlled stages are known to reduce substantially the duration of the transient due to the rapid discharge of electrode and tissue capacitances through the low output impedance of the stage.[38,82] Various approaches described in the literature to obtain output stages suitable for artifact reduction are discussed later.

D. Artifact-Related Characteristics of the Myoelectric Signal Amplifier

The design of the myoelectric signal amplifier can incorporate features that help reduce the sensitivity of the amplifier to stimulus artifacts. Some of these features are

1. A high input impedance (>100 MΩ) renders the amplifier insensitive to the impedance of the skin and enables it to effectively suppress the generation of differential voltages due to common mode excitation when electrode impedances are not exactly equal. Since the stimulation current across the limb generates a large common mode artifact, a high input impedance is desirable to reduce artifact amplitude.
2. Since stimulation current causes a common mode excitation to the differential amplifier, a high (>100 dB) common mode rejection ration (CMRR) is critical for artifact suppression. This characteristic is also important for reducing the effect of common mode line interference on the patient.
3. Stimulation current also produces a differential mode signal between the detection surfaces. This signal is amplified by the front end and may cause saturation of the subsequent stages. In order to avoid this problem, the gain of the front end should generally be kept low ($G < 20$) and other measures should be taken not to saturate subsequent stages.
4. Decoupling of the stimulator reference and power supply from the myoelectric signal amplifier reference and power supply also contributes to artifact reduction. Optical isolators and DC-DC converters are generally used to obtain decoupling.
5. In order to remove the effect of unequal half-cell DC potentials, galvanic skin potentials, and motion artifacts, the myoelectric signal amplifier requires a high-pass filter with a 3-dB corner frequency between 1 and 15 Hz. The stimulation pulse introduces a slow exponential transient in the output of such a filter. The amplitude of this transient may be reduced by decreasing the high-pass corner frequency at the price of a lower rejection of motion artifact and electrode half-cell voltage fluctuations.
6. Capacitive couplings between stimulating and recording leads also contribute to the generation of the stimulation artifact[108] and should be minimized.

E. Artifact Generation Model

A block diagram of the artifact generation model has been reported by McGill et al.[108] A version of this model, slightly modified by Knaflitz,[83] is reported in Figure 5.

The input of the system is represented by either the stimulation current (I_{stim}) or the stimulation voltage (V_{stim}). Since stimulation electrodes have nonlinear impedances (Z_A^*, Z_C^*) when voltage-controlled stimulation is used, the stimulation current is a nonlinear function of the stimulation voltage. The system output is represented by the stimulation artifact filtered by the high-pass filter of the myoelectric signal amplifier, whose time constant is τ. The stimulation

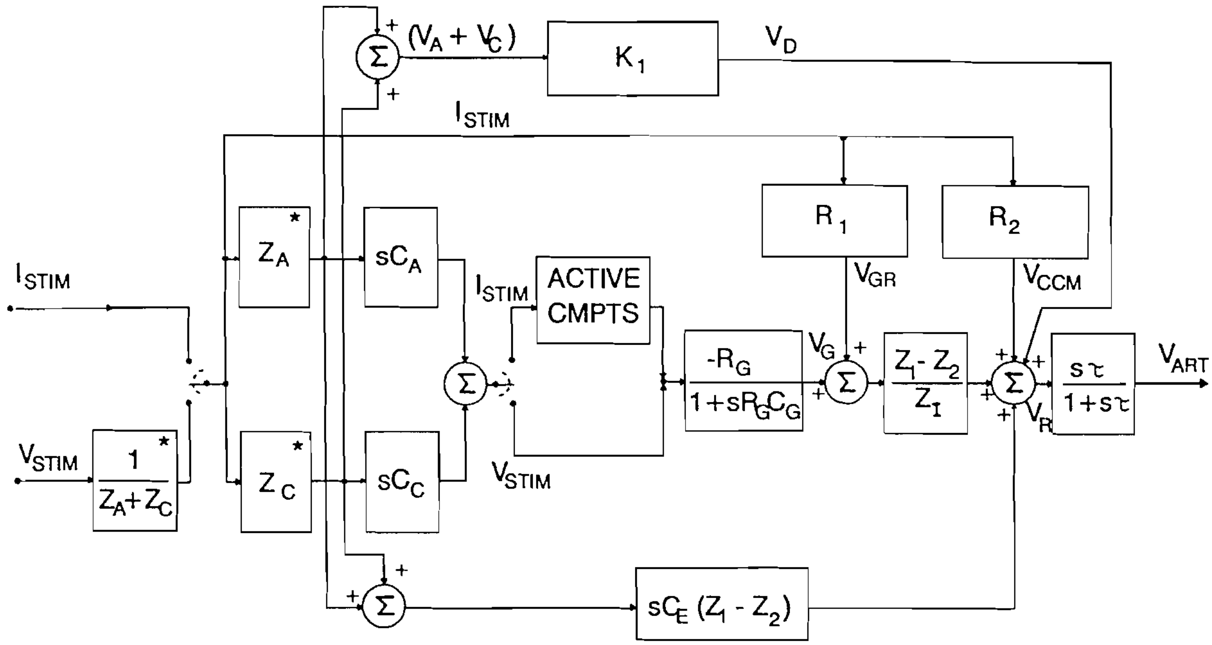

FIGURE 5. Block diagram of the artifact generation model proposed by McGill et al.[108] and slightly modified by Knaflitz.[83] Z_A, Z_C: impedances of stimulation electrodes (nonlinear); C_A, C_C: stray capacitances between the outputs of the stimulator and ground; V_A, V_C: voltage drops between stimulation electrodes and ground; C_E: stray capacitance between stimulating and recording leads; Z_1, Z_2: impedances seen from the inverting and noninverting inputs of the EMG amplifier; Z_I: input impedance of the differential amplifier; ACTIVE CMPTS: this block takes into account the nonlinearity of the term $V_AC_A + V_CC_C$ during current controlled stimulation; R_G, C_G: resistance and capacitance components of the reference electrode impedance; R_1: resistor that simulates the direct contribution of the stimulation current to the voltage spike; R_2: resistor that simulates the direct contribution of the stimulation current to the common mode voltage; K_1: block that takes into account the contribution of the discharge of the tissue and electrode capacitances to the fast tail; τ: time constant introduced by the DC blocking capacitor of the high-pass filter in the EMG amplifier; and *: nonlinear blocks.

artifact is produced by the summation of four components: (1) the artifact component due to the charge and discharge of electrode and tissue capacitances through the resistive components of electrode and tissue impedances, (2) the differential voltage produced by the flow of the stimulation current through the tissue underneath the detection electrode, (3) the differential voltage due to common mode conversion when the input impedances of the myoelectric signal amplifier (Z_1, Z_2) are not identical, and (4) the differential signal due to conversion to differential mode of the capacitively coupled common mode excitation.

The contribution made by the conversion of common mode signals into differential mode signals may be minimized if the input impedances of the differential amplifier are approximately equal and a few orders of magnitude higher than the electrode impedances.

The artifact transient due to the myoelectric signal amplifier high-pass filter may be substantially reduced by using low corner frequencies, and it may be virtually removed by using DC coupling of the myoelectric signal amplifier.

F. Suppression of the Stimulation Artifact

In 1978, Del Pozo and Delgado[38] proposed a *hybrid* stimulator, which was able to combine the advantages of current-controlled stimulation with those of voltage-controlled mode between stimuli. These authors used a field effect transistor to short the output of a current-controlled output stage between stimuli, thus obtaining short transients, although their parameters were not reported in the article. The output pulse was monophasic and could provide a 3-mA to a 10-

kΩ load. While this approach is interesting, the solution is not suitable for transcutaneous stimulators that must provide higher output currents (50 to 100 mA_{pp}) with biphasic output pulses.

In 1981, Spencer[153] proposed an optically isolated, biphasic, current-controlled output stage for artifact suppression to be used for *in vitro* studies. Artifact reduction was obtained by means of integral isolation of the stimulation circuit from ground, and by using true biphasic stimulation. This scheme reduces electrode polarization, which is a relevant source of artifact. Moreover, biphasic stimulation also accelerates the discharge of tissue and electrode capacitances through the stimulator output stage. The author did not provide an example of the artifact suppression capabilities of his device.

Several other authors proposed techniques aimed at reducing the stimulation artifact by introducing specialized circuitry in the myoelectric signal amplifier. In 1971, Freeman[55] proposed a circuit for intracellular signal detection based on a sample and hold amplifier switched to the hold mode during the stimulation artifact. No quantification of the artifact suppression capability of the device was given. In 1975, Roby and Lettich[141] proposed a modified version of Freeman's circuit, including prestimulus blanking capability and the possibility of initiating data collection prior to stimulus delivery, in order to obtain a prestimulation baseline to be used when averaging evoked responses. A similar approach was presented in 1978 by Babb et al.[9] Their device was suitable for EEG recordings and included three artifact suppression techniques: (1) two different front ends, a classic AC coupled stage, and a DC coupled stage were used to eliminate the transient due to the amplifier high-pass filter; (2) the gains of cascaded stages were selected to minimize the risk of saturation; and (3) a sample and hold amplifier with prestimulus blanking capability was used to remove the stimulation artifact. Their device was not isolated from ground, a condition possibly leading to safety and to common mode signal problems. In the same year, Walker and Kimura[158] presented an amplifier featuring a fast recovery time from overload. Their goal was to reduce the transient due to the myoelectric signal amplifier high-pass filter, which allowed a very rapid recovery from possible saturation. This goal was achieved via eliminating coupling capacitors between cascaded stages by establishing a low-frequency cutoff and eliminating electrode DC offset by means of an integrator in a negative feedback loop. Values close to the saturation limits of the amplifiers in the forward chain caused opening of the negative feedback loop, thus eliminating the high-pass filtering effect of the integrator and allowing a very fast (reportedly <1 ms) recovery time from saturation.

Roskar and Roskar[142] proposed a different approach in 1983, consisting of a myoelectric signal amplifier with digitally controlled gain, switched from 1 during stimulation to 1000 between stimuli. Qualitative results appeared satisfactory, but no quantification of the amplifier transient consequent to gain switching was provided. Furthermore, a gain ratio of 1000 may not always be sufficient to obtain an acceptable artifact suppression.

In 1988, Knaflitz and Merletti[82] described a device that featured a hybrid output stage, optical isolation of both the stimulation output stage and of the input of the myoelectric signal amplifier, slew-rate limiting of the signal in the isolated stage, and signal blanking (pre- and post-stimulus) in the ground referred stage. The worst case input-referred artifact was about $25\mu V_{pp}$ for a stimulus duration of 1 ms. Moreover, the input-referred artifact was insensitive to the stimulus amplitude and/or frequency. This device has been intensively used for studying muscle fatigue, muscle fiber recruitment order, and muscle crosstalk.[85,112,114] The main feature of the output stage is its ability to function as a current generator during stimuli and as an active short circuit between stimuli. The basic idea differs from that proposed by Del Pozo and Delgado[38] since they used a field effect transistor to implement a passive short circuit. This is effective only with monophasic stimulation pulses, while switching the output stage from current to voltage-controlled mode is suitable for either mono- or biphasic stimulation pulses. A block diagram of the stimulation output stage is presented in Figure 6A. Figure 6B shows the performance of the stage when the mode is switched from current feedback (during the stimulus) to voltage feedback (between stimuli) and when the mode is set to current

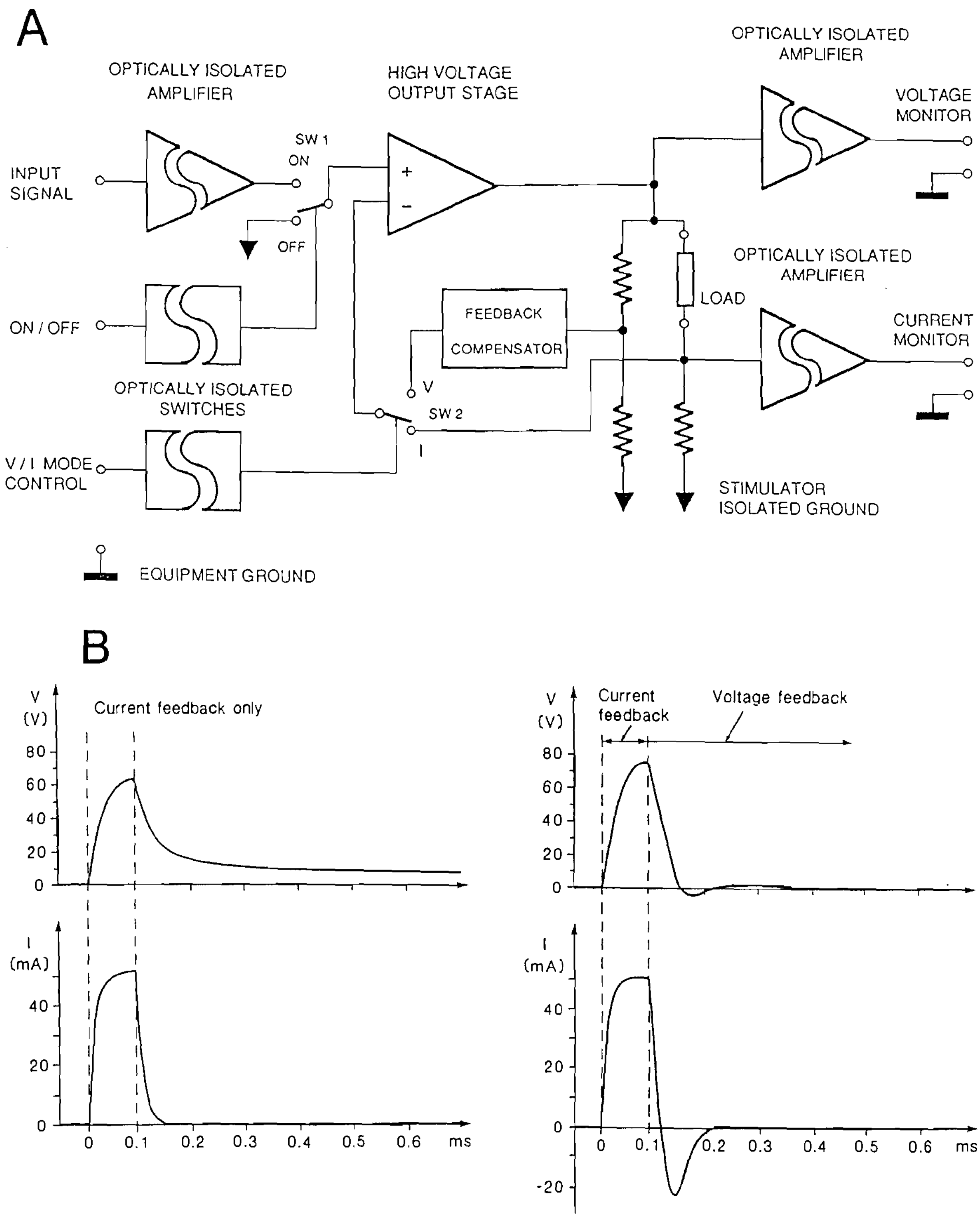

FIGURE 6. (A) Block diagram of the output stage of the hybrid stimulator described by Knaflitz and Merletti.[82] (B) Comparison between the voltage and current outputs obtained from a hybrid output stage (right) and from the same circuit always kept in current controlled mode (left). The hybrid stage allows for a faster decrease of voltage between stimulating electrodes. The current stimulus is no longer strictly monophasic and the negative phase is due to the discharge of the electrode and tissue capacitances.

feedback only. The latter case clearly shows the long voltage transient, a fraction of which would be present between the detection electrodes.

In order to obtain a satisfactory reduction of the stimulation artifact, several factors were implemented:

1. The output stage of the stimulator was operated in the hybrid mode, resulting in a shorter transient, as shown in Figure 6B and indicated schematically in Figure 7B.
2. The gain of the front end DD amplifier was limited to 20 in order to avoid saturation due to spikes synchronous with the stimuli.
3. The amplitude of the stimulation artifact and its rise time were reduced by a slew-rate-limiter providing an input-referred limit slope of 5 V/s, a slope larger enough to accommodate maximal M-waves as well as voluntary myoelectric signals. The resulting signal is indicated schematically in Figure 7C.
4. The residual stimulation artifact was removed from the output signal by means of CMOS switches activated during a time window that included the stimulus and was continuously adjustable between 0.5 and 5 ms after the end of the stimulus. The resulting signal is indicated schematically in Figure 7D.

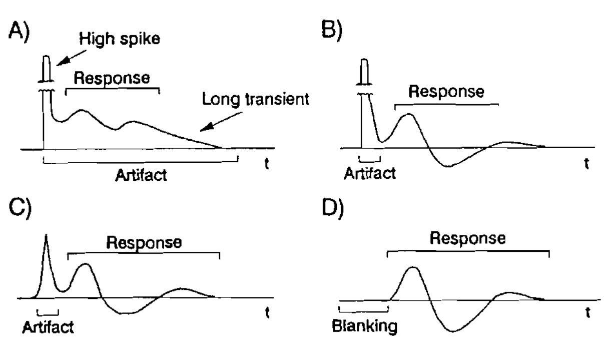

FIGURE 7. Effect of the artifact suppression techniques proposed by Knaflitz and Merletti.[82] (A) Signal recorded without any artifact removal technique. (B) Signal recorded with hybrid stimulation. The artifact long-tail is substantially reduced. (C) Signal recorded with hybrid stimulation and slew rate limiting. The spike is lowered to avoid saturation. (D) Signal recorded as in (C) with residual artifact blanking obtained by time windowing. The suppression of the artifact is virtually complete.

A block diagram of the detection and signal conditioning system is shown in Figure 8A. The effect of this technique for the suppression of the stimulation artifact is depicted in Figure 8B, which shows signals recorded during the stimulation of a motor point of the human tibialis anterior.

Recently, Blogg and Reid[19] published a digital technique for stimulation artifact reduction. Their system was designed mainly for performing studies on the hamster diaphragm stimulated either via the phrenic nerve or by means of platinum electrodes directly placed on the diaphragm. Myoelectric signals obtained with monopolar technique were conditioned by means of a DC-coupled amplifier and converted by means of a 12-bit A/D board. The artifact reduction technique was implemented in software. The authors did not provide quantitative assessment of the artifact reduction capability of the system. Results presented in their work show that their system is able to reduce substantially the long and short tail of the stimulation artifact, but its ability to remove the spike synchronous with the stimulus appears to be rather poor.

V. EFFECT OF STIMULATION WAVEFORMS AND ELECTRODE PROPERTIES

The effects of a particular stimulation waveform on the electrical and/or mechanical muscle response have not yet been clarified adequately. The shape of the stimulation pulse might modify the myoelectric signal by affecting the pool of activated motor units. Although some waveforms are known to have inhibitory, rather than excitatory, effects when applied directly to a nerve trunk by means of cuff electrodes,[1,5,13,22,52,53,152] the information available on the effect of different waveforms applied by means of surface electrodes is very limited and focuses mostly on pain tolerance, selectivity of different waveforms, and energy efficiency.

A. Pain Tolerance

The issue of pain or discomfort due to surface electrical stimulation is not directly related to myoelectric signals, nevertheless, it becomes relevant if sustained electrically evoked contrac-

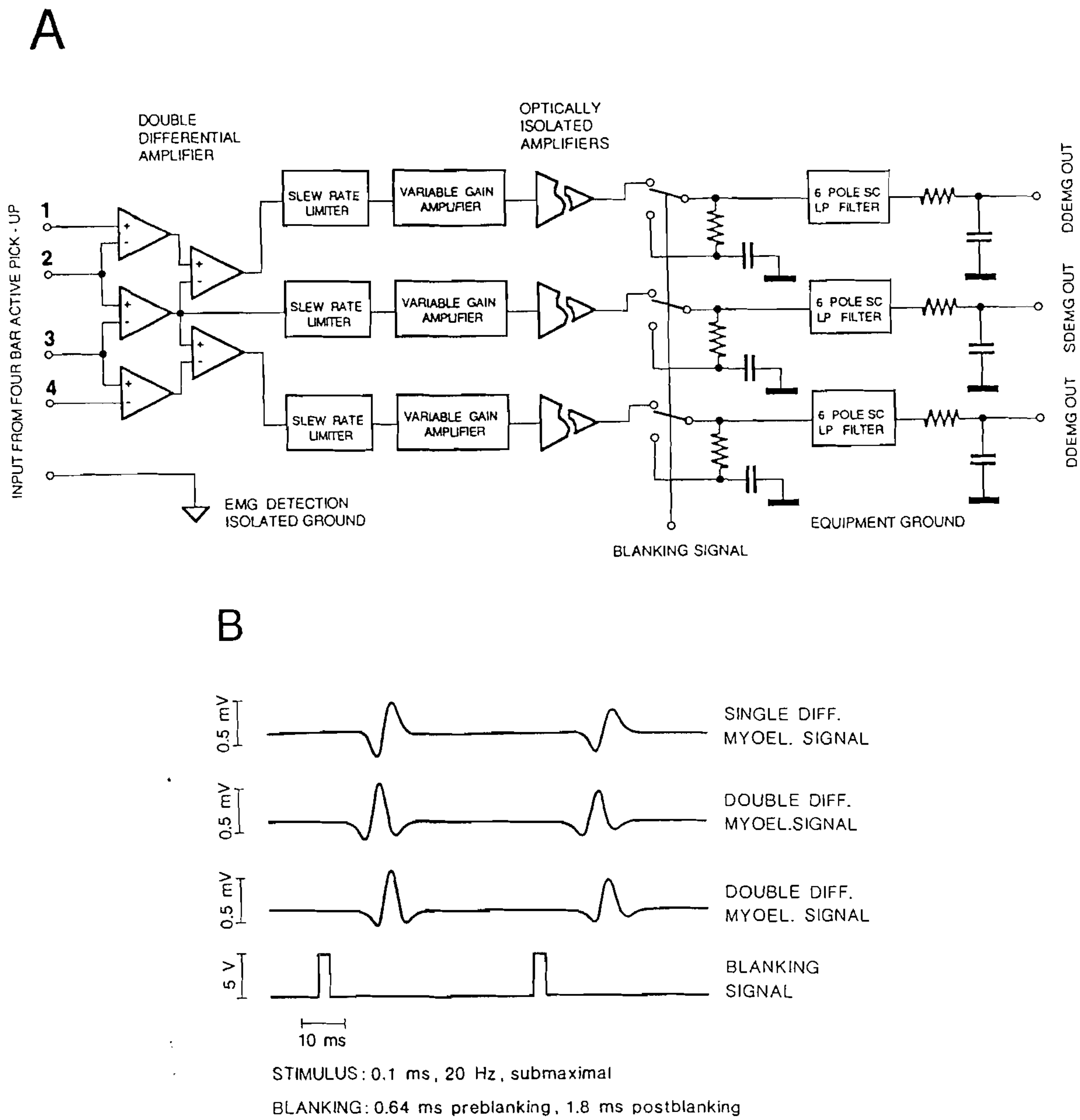

FIGURE 8. (A) Block diagram of the EMG amplifier input stage proposed by Knaflitz and Merletti.[82] (B) Example of SD and DD signals recorded during supramaximal stimulation of the human tibialis anterior muscle. Each blanking pulse (fourth trace) includes a 0.64-ms preblanking pulse, the stimulation pulse, and a 1.8-ms postblanking pulse.

tions must be induced. The early work of Milner and Quambury[120] suggested that pain is related to the peak current and not to the electrode size. In 1973, Gracanin and Trnkoczy[65] studied electrical stimuli of different shapes with or without DC offset and observed that: (1) stimulation pulses lasting 0.3 ms were more tolerable than those lasting 1 ms, (2) the current-controlled stimulation mode was less comfortable than the voltage controlled mode, (3) 50 Hz was the preferred stimulation frequency, (4) monophasic stimulation with no DC component added was less painful than biphasic stimulation, and (5) most subjects were not able to find any difference between sensations induced by rectangular and exponential stimuli. They concluded that pain depends mainly on the electric charge that flows through the tissues during stimulation, while the shape of the stimulus and the DC offset introduced are irrelevant.

Bowman and Baker[21] performed a number of experiments to verify and extend the data reported by Gracanin and Trnkoczy.[65] Twelve subjects were asked to compare stimuli of different durations, while 11 others compared stimulation modes and waveforms (rectangular pulses — symmetric and asymmetric). Large conductive rubber electrodes were placed above the quadriceps. Stimulus amplitude was regulated to obtain an extension torque at the knee joint approximately equal to 20% MVC. These authors found that: (1) stimulation pulses lasting 0.3 ms were less painful than pulses lasting 50 μs, (2) biphasic pulses (charge balanced) were preferred to monophasic asymmetric pulses, and (3) voltage-controlled stimulation was reportedly less painful than current-controlled stimulation. Three years later, McNeal and Baker[107] observed that electrode size had little effect on moments produced by the quadriceps muscle with either mono- or bipolar stimulation. Biphasic stimulation produced higher moments than monophasic stimulation (+20 to 30%) and monopolar cathodic stimulation produced higher moments than monopolar anodic stimulation.

Mason and McKay[102] carried out experiments on the upper limbs of several volunteers to correlate pain sensation experienced by the subjects and the electrical parameters of the skin. They reported that, when metal electrodes were used without conductive gel between the electrode surface and the skin, subjects perceived two different pain sensations: an acute soreness was felt at relatively low stimulation levels (≈500 μA with rectangular biphasic pulses lasting 1 ms) and vanished after approximately 30 s of stimulation, while a burning sensation appeared when the stimulation intensity was increased above 5 to 10 mA. The authors concluded that pain is not associated with dissipation of electrical energy inside the tissues, but probably with direct excitation of free nerve endings in the skin. They also concluded that the use of conductive gel is recommended to avoid pain when exposed to low current levels.

Alon[4] and Alon et al.[3] found that the most suitable range for motor stimulation with rectangular monophasic pulses is between 50 and 200 μs and the greatest nonpainful torque can be obtained from the triceps brachii, with pulse widths in the neighborhood of 100 μs. They also found that motor responses can be evoked with pulse charge densities in the range between 0.5 and 0.25 μC/cm^2, the lower values corresponding to electrodes with an area of 81 cm^2 and the higher values to electrodes with an area of 9 to 36 cm^2.

B. Selectivity of Different Waveforms

The ability to selectively excite axons with different stimulation thresholds is of paramount importance in studying the behavior of different populations of motor units.

Gorman and Mortimer[62] investigated the issue of stimulation selectivity using the Frankhenhauser-Huxley model of myelinated fibers. They simulated two different axons, with diameters of 10 and 20 μm, respectively, placed at a certain distance from the stimulation electrode, yielding a stimulation threshold equal to 1 mA. The stimulation pulses were rectangular, biphasic, charge balanced, and with the two phases separated by a delay. The phase duration of stimuli ranged from 25 to 200 μs, while the delay was progressively increased from 0 to 80 μs. The authors found that the greatest difference between the stimulation thresholds was achieved by using narrow stimuli and short delays between the two phases. In particular, fiber selectivity was primarily affected by the phase duration, whereas variations of the delay in the range 40 to 80 μs led to negligible changes in the threshold difference between the simulated fibers. Three years later, Gorman and Mortimer[63] carried out experiments to verify the simulated results. Electrodes were placed on the nerve trunk at approximately 10 mm from the innervation zone of the gastrocnemius muscle of 15 cats, and isometric force developed by the muscle during electrical stimulation was measured. Results were in good agreement with simulations. Moreover, the authors demonstrated that the slope of the *recruitment curve* (normalized force vs. stimulation current) decreases by using short stimulation pulses, thus allowing a more controllable recruitment of motor units.

The recent work of Fang and Mortimer[52,53] indicates the potential of quasitrapezoidal waveforms applied to a tripolar nerve cuff electrode to achieve selective stimulation of small motor axons and to obtain physiological recruitment order of motor units in an electrically activated muscle.

C. Energy Efficiency and Electrode Properties

The minimization of stimulus energy is desirable in order to: (1) reduce the probability of skin damage underneath the electrodes, and (2) increase the endurance of power sources in portable stimulators. Crago et al.[34] studied energy dissipation underneath the stimulation electrodes and found that rectangular pulses require a larger amount of energy than increasing exponentials. Unfortunately, increasing exponential pulses are not easy to generate.

Commercially available surface electrodes are made of conductive rubber, sponge material, "karaya" resin, etc. They may or may not require conductive paste, they may be self-adhesive or fixed with straps. For FES applications, they may even be incorporated in garments. A comparison among the most common electrode types has been carried out by Nelson et al.[130] The shape of the electrode may have some relevance with respect to selectivity since current density is higher near the edges of the electrode.[23] In general, the relevance of surface electrode shape and stimulation waveform shape with respect to spatial or fiber type selectivity is not well assessed and requires further investigation.

VI. PARAMETERS AND PROCESSING TECHNIQUES OF THE ELECTRICALLY EVOKED MYOELECTRIC SIGNAL

A number of time and frequency domain attributes have been used to describe the myoelectric signal. This section reviews some basic concepts related to the computation of these attributes for voluntary and electrically evoked signals.

From a statistical point of view, the myoelectric signal obtained during voluntary isometric contractions at constant force may be considered as a bandlimited stochastic process with Gaussian distribution of amplitudes.[14] Stationarity evaluation is of paramount importance for spectral estimation of myoelectric signals. In fact, the power spectral density function (PSD) is defined for *wide-sense stationary* signals only.[133] In most cases, during relatively low level and short contractions (20 to 30% MVC, up to 20 to 40 s), the myoelectric signal may be considered wide-sense stationary.[11,133] When the contraction level is increased, the wide-sense stationary hypothesis holds during shorter epochs[11] (0.5 to 1.5 s at 50 to 80% MVC). The time course of time and frequency domain attributes is generally computed by subdividing the signal in epochs during which the wide-sense stationary hypothesis holds, and then by computing the values of the selected attributes over each epoch. Signal attributes will then be functions of time and will be referred to as "variables".

The raw periodogram is the spectral estimation technique most frequently adopted for voluntary myoelectric signal. After segmenting the signal in epochs in which the wide-sense stationary assumption holds, the PSD function is computed by taking the square of the modulus of the discrete Fourier transform of the signal, which is generally computed by means of the radix-2 fast Fourier transform (FFT) algorithms. The raw periodogram gives a spectral estimate in which the single spectral line is affected by a standard deviation of 100%; heavy smoothing (with consequent loss of resolution) is required to reduce the random fluctuations (see Figure 9A). In most applications of surface electromyography, however, the power spectrum is estimated mainly to extract spectral variables. Due to the statistical properties of the estimators of the spectral variables of interest in myoelectric signal processing, the raw periodogram is satisfactory in most applications.

Different techniques are generally used to estimate the PSD function of voluntary or electrically evoked myoelectric signals. Electrically evoked signals may be considered deterministic and quasiperiodic with period determined by the stimulation frequency imposed by the stimulator (see Figure 1B). Three different strategies may be used to compute the attributes of the signal in this case:

1. The signal is subdivided in epochs during which M-waves may be considered time invariant, and then amplitude and frequency

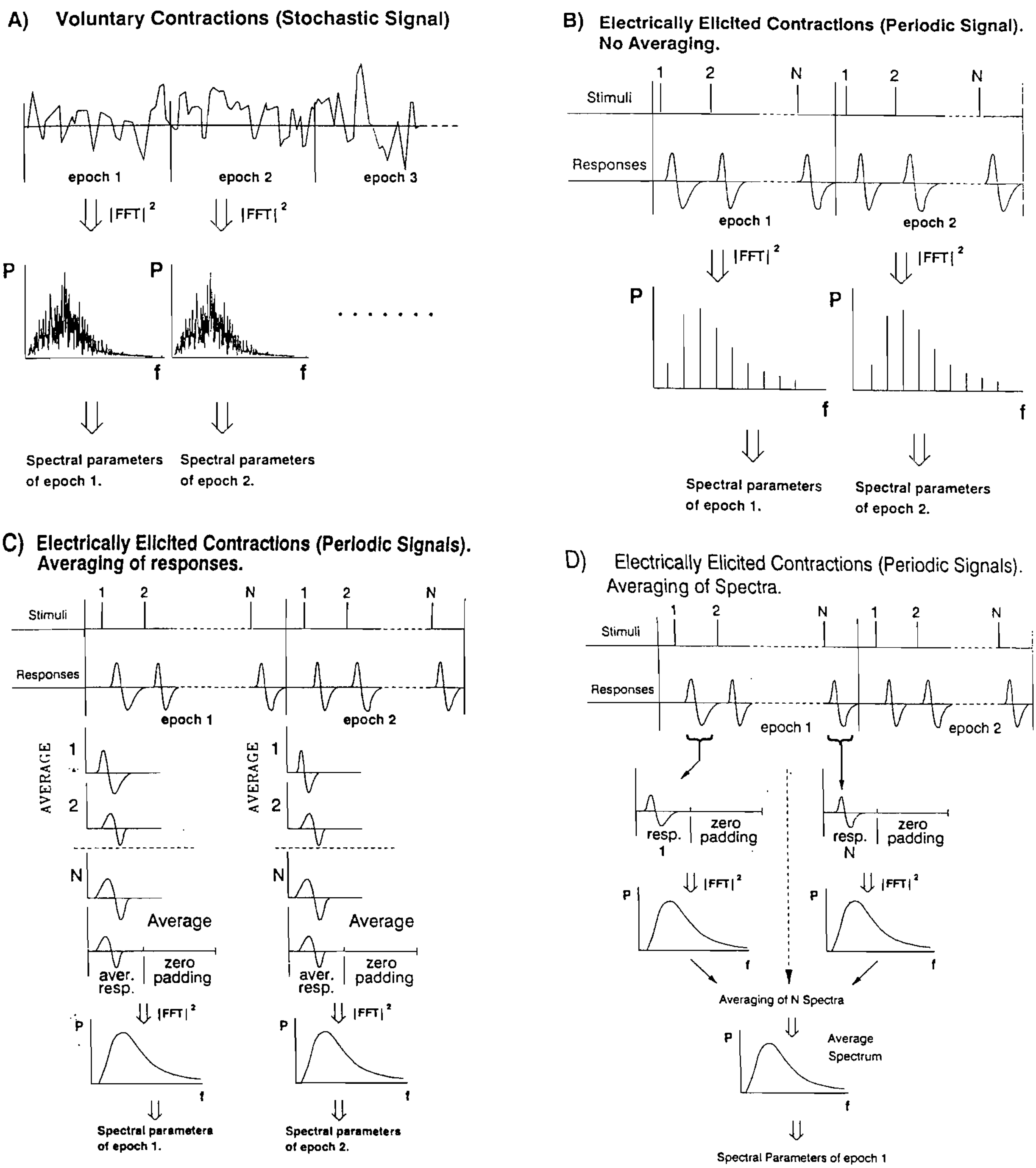

FIGURE 9. Estimation of myoelectric signal spectral variables. (A) Spectral estimation during voluntary contractions. The signal is divided into a sequence of contiguous segments (epochs) during which the signal is assumed to be stationary. The power spectral density function is estimated by fast Fourier transform (FFT) and spectral variables (mean frequency, MNF; median frequency, MDF) are computed for each epoch. Acceptable epoch durations are between 0.5 and 2 s, depending on the level of contraction. Spectral values have large variance and are separated by $1/T_e$ where T_e is the epoch duration. (B) If the same technique described in (A) were used for electrically evoked (quasiperiodic) signals, spectral values (lines) would be separated by f_s where f_s is the stimulation frequency. Spectral resolution would be unacceptable. (C) The power spectral density function of a stimulus-triggered waveform may be computed by averaging N responses, adding zeroes to the averaged waveform up to time T (zero padding), and then computing the FFT of the resulting time sequence. Spectral values will be separated by $1/T$. (D) The power spectral density function of each stimulus-triggered waveform may be computed, after zero padding up to T, and the resulting N spectra may then be averaged to provide a power spectral density function estimate with resolution $1/T$.

attributes are computed over each epoch. In this case, if the repeated epoch is periodic, the PDS function will be discrete and the spectral lines will be spaced by a frequency interval equal to the stimulation frequency (see Figure 9B).

2. The PSD function, frequency, and amplitude attributes are computed over each individual M-wave considered to be a finite energy signal with limited support in time. In this case, the PSD function will be continuous and a set of attributes will be obtained for each M-wave. In this case, stationarity is irrelevant. Moreover, since each single M-wave is processed, the computational cost of this approach is generally high, and the time series of the computed attributes reflects random variations of the M-wave. The spectral density of the signal may be interpolated by means of zero padding in the time domain[132] to obtain the desired spacing between contiguous spectral lines (see Figure 9D).
3. The signal is subdivided in epochs, during which M-waves may be considered to be time invariant (as in case 1), and then the average M-wave is computed over each epoch. Amplitude and spectral attributes are then computed on the average M-wave. This approach combines the advantages of methods (1) and (2). In fact, as in case (2), the average M-wave may be considered to be a finite energy, having limited support signal, therefore, its PSD function is continuous. Moreover, signal attributes are computed on a single data sequence for each epoch, thus reaching a high computational efficiency. Finally, because of the averaging process, the signal-to-noise ratio will be improved by the square root of the number of M-waves averaged in each epoch. The spectral density may be interpolated by means of zero padding in the time domain as in case (2) (see Figure 9C).

Among the time domain variables are the *average rectified value* (ARV), the *root mean square value* (RMS), the *muscle fiber* CV, *peak* and *peak-to-peak amplitude, duration,* and *area* of the M-wave. Among the frequency domain variables are the *mean* (MNF) and *median* (MDF) *frequency* of the myoelectric signal PSD function. The values and the time course of these variables reflect physiological correlates and have been used to detect or monitor pathologies and to describe neuromuscular properties.

A. Amplitude Parameters

The quantitative description of electrically evoked motor responses has received limited attention in the literature. A variety of parameters have been used. Among these are the peak-to-peak amplitude, the duration (defined either as the time interval from the beginning to the end of the M-wave or as the time interval between the positive and the negative peaks of the M-wave), the integral of the evoked potential (area of the M-wave), and the product of duration times of the peak-to-peak amplitude.[56]

Considerable confusion and difficulty surround the definition of wave duration, mean value, and other signal attributes. Thus, it is prudent to use general concepts of signal analysis rather than concepts developed for the specific case. The standard amplitude parameters commonly used in classical signal processing applications are the ARV and the RMS. The ARV is the area between the rectified signal and the time axis (signal integral) computed during a time interval T and divided by T, therefore providing a mean voltage value. RMS is obtained by dividing the energy of the signal during a time interval of duration T by the value of T, thus providing a mean power value whose square root is the RMS value. Both parameters imply integration over the time interval T, and as long as T is greater than the duration of the evoked response and noise is negligible with the respect to the signal, the value of T affects ARV or RMS only as a proportionality constant. Moreover, if T is chosen as a multiple of the period of the myoelectric signal, and the myoelectric signal may be considered as time invariant in T, the value of T does not affect the estimates of the values of ARV and RMS. Mathematical expressions of the ARV and the RMS value are reported below:

$$v_{arv}(t) = \frac{1}{T}\int_{-T/2}^{T/2} |v(t)|\, dt \tag{5}$$

$$v_{rms}(t) = \sqrt{\frac{1}{T}\int_{-T/2}^{T/2} v^2(t)\, dt} \qquad (6)$$

B. Frequency Parameters

Frequency parameters of the M-wave have received even less attention than the amplitude parameters. The work of Kranz et al.[89] and Mills[119] has indicated that the spectrum of evoked myoelectric signals does not differ significantly from that of voluntary signals, except for the different variances of the estimates due to the stochastic nature of the second signal and to the deterministic nature of the first. Two main frequency parameters have been used to describe the spectrum of the myoelectric signal, i.e., its MNF (or centroid) and MDF. The use of the MNF was introduced by Lindstrom and Magnusson[97] and the MDF by Stulen and DeLuca.[156]

The PSD MDF is defined as the frequency that divides the power spectrum in two regions having the same amount of power. The mathematical expression for the median frequency MDF is

$$\int_0^{MDF} P(f)\, df = \int_{MDF}^{\infty} P(f)\, df = \frac{1}{2}\int_0^{\infty} P(f)\, df \qquad (7)$$

The MNF (or centroid) is defined by:

$$MNF = \frac{\int_0^{\infty} fP(f)\, df}{\int_0^{\infty} P(f)\, df} \qquad (8)$$

The first step toward the computation of spectral variables is the estimation of the PSD function of the signal. When the voluntary myoelectric signal is processed (albeit the raw periodogram is an asymptotically unbiased but inconsistent spectral estimator), both spectral variables (MNF and MDF) are computed adding the amplitudes of many spectral lines, thus dramatically reducing the effect of the indetermination of the power content of the individual spectral lines. Generally, the raw periodogram allows estimation of MNF and MDF values with a standard deviation of only a few percent, despite the 100% standard deviation of the amplitude of each spectral line. Estimates of MNF and MDF are also affected by a standard deviation that increases with decreasing epoch duration.[12] The proper choice of the epoch duration is conditioned by the nonstationarity of the signal, by the desired frequency resolution, and by the acceptable standard error of the parameters to be computed. Commonly used epoch durations range from 0.5 to 2 s, the shortest being used for intense contractions with highly nonstationary signals.

Due to the characteristics of the PSD function of the electrically evoked myoelectric signal, the estimate of the spectral density is far more accurate than that obtained from voluntary signals. MNF and MDF are the most suitable parameters to track spectral compression due to localized muscle fatigue. MDF has been shown to be less sensitive to added white noise;[156] in contrast, MNF may generally be estimated with a lower relative error.[12,74] Theoretically, both MDF and MNF are equally sensitive to spectral compression, whereas a different rate of change indicates a change of spectral shape (see Appendix for details). However, often in practice, the MDF has been found to be more sensitive to modifications that occur in the myoelectric signal during sustained voluntary contractions[112] (see Figure 14).

C. Conduction Velocity

Muscle fiber CV is a basic physiological parameter, and it is known to be related to the type and diameter of muscle fibers,[72] to ion concentration in different compartments, to pH of intracellular and interstitial fluids,[24] and to motor unit firing rate or stimulation frequency.[118,123] Measurement techniques and clinical applications were discussed in a 1989 article by Arendt-Nielsen and Zwarts.[8]

Several different methods have been presented in the literature to estimate CV by means of surface electrodes. Those most frequently used are listed below, and their advantages and drawbacks are discussed briefly.

1. Spectral Dips Technique

This method was first introduced by Lindstrom and Magnusson.[97] When a surface myoelectric signal is detected by means of a pair of electrodes in a differential configuration, the spectral components of the signal are modified by the spatial filtering effect of the detection electrode (see Section III). The power spectrum of the signal is multiplied by the square modulus of the electrode transfer function, whose expression is

$$|H(f)|^2 = K\left(\sin\frac{\pi f d}{v}\right)^2 \tag{9}$$

where: $|H(f)|$ = module of the transfer function of the detection electrode, K = proportionality constant, f = frequency, d = interelectrode distance, and v = muscle fiber CV.

As mentioned in Section III, the transfer function of the detection electrode will be zero when $fd/v = N$, with $N = \pm 1, \pm 2, \pm 3, \ldots$. Consequently, the CV may be estimated by measuring the frequency at which the first dip occurs and then multiplying it by the interelectrode distance. This method is rarely applied in practice because (1) for typical interelectrode distances of 5 to 10 mm the first dip occurs in the high-frequency range, where the power associated to the myoelectric signal is close to zero; and (2) when studying the myoelectric signal obtained during voluntary contractions, the variance of the spectral estimate does not allow reliable detection of the spectral dips.

2. Cross-Correlation Technique

This technique has been described in detail in several papers (see References 129, 146, and 163, among others) and is currently used by a number of researchers. Figure 10 shows a schematic representation of the principles on which this technique is based. Surface myoelectric signals are collected at two different sites along the active muscle fibers. If the system is assumed to be space invariant within the detection area of the electrodes, the two signals $x(t)$ and $y(t)$ result,

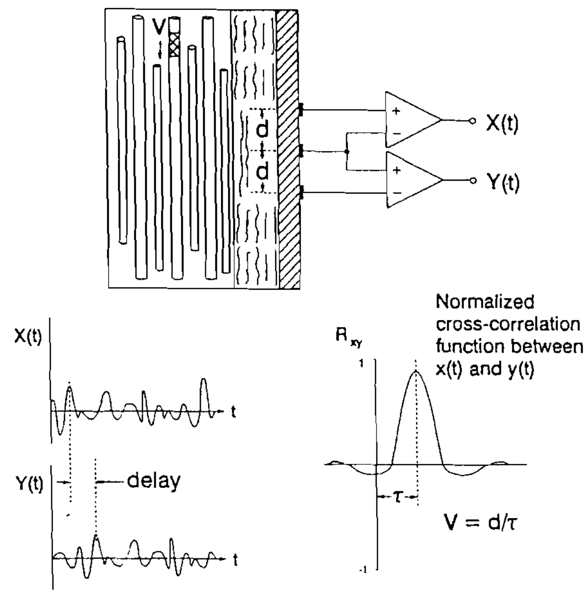

FIGURE 10. Estimation of time delay between two myoelectric signals by means of the cross-correlation function. $X(t)$ and $Y(t)$ may be two SD signals, as indicated in this figure and in Figure 2B, or two DD signals, as indicated in Figure 2C.

time-shifted by the time interval $\Delta\tau = d/v$, (d = interelectrode distance, v = CV). If the two signals are equal but time delayed with respect to each other, the peak of their cross-correlation function (normalized with respect to the product of the standard deviations of the two signals) has a unity value and its position on the time axis provides the delay between the two signals. The DD technique[25] described in Section III and displayed in Figure 2C is particularly suitable for this application because it allows cancellation of the nontraveling SD signals common to all electrode pairs. If the two signals are not equal, the peak of the normalized cross-correlation function is <1 and its value may be taken as an indicator of the quality of the estimate of CV. For voluntary contractions, acceptable values are above 0.70, whereas for electrically evoked signals, values >0.90 are usually obtained.

In order to obtain acceptable resolution in the CV estimate for typical interelectrode distances (5 to 20 mm), the time delay must be computed with a resolution of 10 to 20 μs. Such a resolution may be obtained by oversampling the signals or by interpolating the cross-correlation function. Oversampling is burdensome from the point of view of computational time and memory allocation. (A resolution of 10 μs may be obtained with a sampling frequency of 100 KHz, yielding an oversampling factor of about 100.) Interpolation with a suitable function may be performed near the maximum of the cross-correlation function, thus increasing the computational efficiency.[163]

3. Spectral Matching Technique

This technique is theoretically equivalent to the cross-correlation approach, but the computation of the time delay between the two signals is performed in the frequency domain. In fact, it can be shown that minimizing the mean square error between the two signals in the time domain corresponds to minimizing the mean square error between their Fourier transforms.[109] The advantage of working in the frequency domain is found in the ability to shift a signal by a fraction of the sampling period simply by multiplying its Fourier transform by $e^{j2\pi f\Delta\tau}$, with $\Delta\tau$ as the time shift. The search for the minimum of the mean square error between the Fourier transforms may then be performed without either oversampling or interpolation.[109]

A detailed comparison between cross-correlation and spectral matching techniques was presented in 1990 by Bonato et al.[20] These authors demonstrated that the two methods have a very similar sensitivity to quantization error and PSD shape, but spectral matching is slightly less sensitive to added white noise than cross-correlation in the time domain. Spectral matching gives reliable estimates of CV even with signal-to-noise ratios as low as 2. From a computational point of view, spectral matching is definitely less expensive than cross-correlation, usually reducing the computation time by a factor of 10.

4. Other Methods

Some other methods have been proposed in order to obtain the noninvasive estimation of CV. Although these methods are not as widely used as cross-correlation or spectral matching techniques, they offer some advantages and deserve attention:

- Gradient threshold zero crossing method[103]
- Phase response method[78]
- Impulse response function[36,78]
- Time domain interpolation and alignment[159]

The time domain interpolation and alignment technique seems to provide results comparable to the spectral matching technique at a lower computational cost if the waveforms are strongly correlated. A technique to estimate the probability density function of muscle fiber CV has been proposed by Davies and Parker.[36] An estimate of this function may also be obtained with the phase and impulse response function techniques, as suggested by Hunter et al.[78] A quantification of the reliability of this interesting technique applied in real situations is not yet available in the literature.

VII. PHYSIOLOGICAL SIGNIFICANCE OF MYOELECTRIC SIGNAL VARIABLES

An electrically stimulated muscle may be thought of as a giant motor unit whose surface MUAP is the sum of many synchronous MUAP. The contribution of each MUAP to the surface detected signal is affected by a number of geometric and physiological factors whose role is important during either voluntary or electrically evoked contractions. It may be interesting to investigate to what degree electrical stimulation might provide the means for identification, separation, and quantification of any of these factors. Figure 11 provides a schematic representation of the most important factors, but may still be far from including all of them. This representation is a revision of that which originally appeared in the book *Muscles Alive*, by Basmajian and DeLuca (1985). Three major groups of factors may be identified: geometric factors, factors determining the mean and probability density function of CV, and factors determining the length and potential distribution of the depolarized zones of the muscle fibers. The second and third factors relate to the fiber constituency of the active motor unit pool, to blood flow, and to ionic shifts across

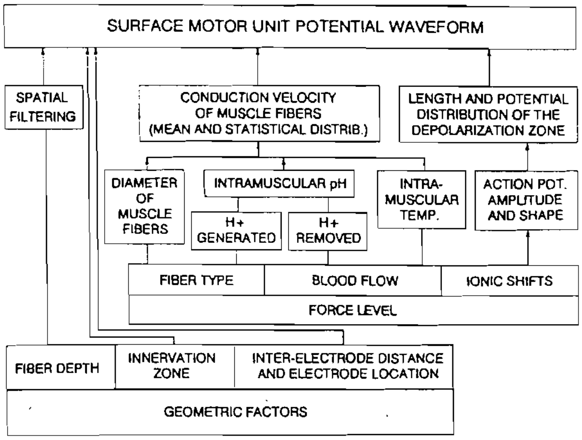

FIGURE 11. Schematic diagram of the most important physiological and experimental factors determining the surface MUAP. An electrically stimulated muscle may be thought of as a giant motor unit whose surface MUAP is the sum of the contributions from many synchronous MUAP.

the muscle fiber membrane; all of these factors are ultimately related to the level of activation of the muscle.

Geometric factors relate to the tissue and electrode system spatial filtering,[97] the electrode location with respect to the innervation zone and the tendons,[143] the width of the innervation zone, and the resulting spatial and temporal scatter of single fiber action potentials.[97]

If geometric factors are assumed to be time invariant during a sustained contraction, the detected signals are functions of the sources of electric field and of their CV. CV, MDF, and MNF are functions of muscle fiber diameter,[72,96] intramuscular temperature,[110,138] and intra- and extracellular pH.[24] Hydrogen concentration (pH) is related to the generation and removal rates of H^+. The generation rate of H^+ is a function of the type, number, and firing rate of active fibers, whereas H^+ removal is related to blood flow which is a function of intramuscular pressure and, therefore, of contraction level. Muscle fiber membrane properties are affected by the concentration gradients of Na^+, K^+, H^+, and several other ions, therefore, the action potential spatial (and temporal) waveshape and length (and duration) are affected by the same factors. During sustained contractions, intramuscular pH and ionic gradients change, leading to changes of action potential spatial length and shape, temporal duration and shape, amplitude, and CV, and eventually resulting in modifications of the surface MUAP or M-wave. In addition to these factors, the active motor unit pool may change during a sustained contraction due to the recruitment or derecruitment of some motor units.

A. Relationship among Spectral Variables, Conduction Velocity, and Length of Surface Potential Distribution

If we consider a single muscle fiber, it can be shown that a decrease of CV results in a time expansion of the detected signal and of its autocorrelation function, as well as in a frequency compression (and amplitude scaling) of its power spectrum (see Appendix and Figure 12). In such a case, the percent of variations of CV, MDF, and MNF is identical. They are also identical and opposite to those of the first zero crossing of the autocorrelation function[84] (see Appendix). In particular, graphs of normalized MNF vs. normalized MDF or of normalized CV vs. normalized MDF would have unity slope and zero intercept.

If this concept is extrapolated to the activated muscle portion, which during stimulation behaves as a single motor unit, the slope and the correlation coefficient of the linear regression of normalized MNF vs. normalized MDF could be taken as an indicator of spectral compression due to time scaling. Near unity values would suggest but not prove spectral compression without change of shape. The addition or removal of motor units would likely change the shape of the signal and of its power spectrum, thereby altering either the linearity or the slope of the relationship between normalized MNF and MDF.

In their work on the human tibialis anterior, the authors have generally found a highly linear relationship between MNF and MDF in electrically evoked contractions that showed progressive PSD compression with no substantial change in shape. During voluntary contractions, visual observation of spectral compression and/or change of spectral shape is made difficult by the large variance of spectral estimates requiring a degree of smoothing which modifies spectral shape and reduces frequency resolution. The linear, unity slope relationship between normalized MNF and

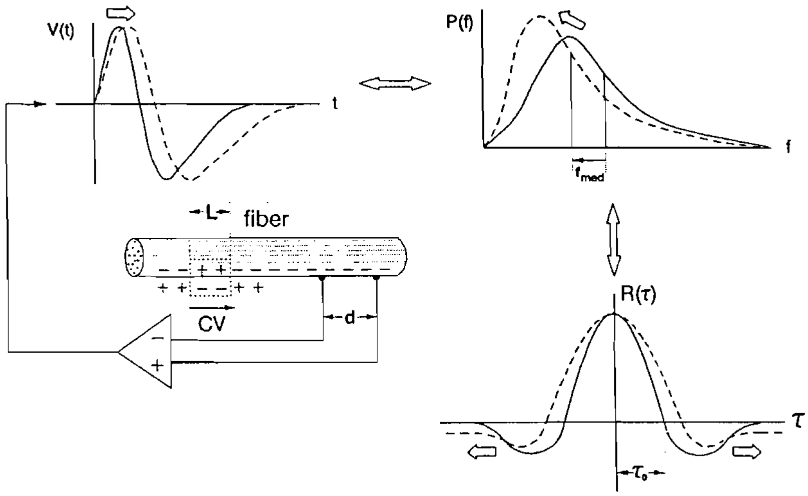

FIGURE 12. Schematic representation of the waveform, of the power spectrum, and of the autocorrelation function of the differential signal detected between two extracellular electrodes placed on or near a muscle fiber. Qualitatively similar signals are obtained from surface electrodes placed above an electrically activated muscle. During a sustained contraction, the waveform progressively expands in time (time scaling), the power spectrum compresses (frequency scaling), and the autocorrelation function expands (mathematical details are provided in the Appendix).

MDF does not seem to hold to the same degree during voluntary contractions as it does during electrically evoked contractions.

Figure 13 shows four different examples of spectral change during sustained contractions. The second spectrum of Figure 13A (voluntary contraction) shows a decrease of power in the high frequency portion rather than compression; the second spectrum of Figure 13B shows a clear case of pure compression and no change of shape with respect to the first spectrum. Figure 13C and D show cases of compression associated with changes of shape. Figure 14 shows how this information may be presented in more compact form by plotting normalized MNF vs. normalized MDF. A linear regression with near unity slope, near zero intercept, and near unity correlation coefficient between these two variables is a necessary but insufficient condition to indicate spectral compression (see the Appendix for details). If spectral compression were caused exclusively by equal percent changes of all CV values, a linear regression with near unity slope, near zero intercept, and near unity correlation coefficient between CV and either MDF or MNF would be expected. Deviation from this relationship would be indicative of the effect of other factors. Although additional research is needed to assess the exact physiological meaning of these observations, it may be speculated that changes of spectral shape are indicative of changes of physiological variables other than average CV. This condition may be easily and clearly detected during electrically evoked contractions that allow for the resolution of small changes, whereas the stochastic nature of the signal makes it difficult to detect it during voluntary activation.

The work of Brody et al.[24] on the electrically stimulated hamster diaphragm has demonstrated that CV and spectral variables change by the same percentage (about 15%) when extracellular pH is decreased from 7.4 to 6.6. This study conclusively proved that a change in the extracellular pH affects the spectral variables of the surface myoelectric signal through the effect it has on the CV of the muscle fibers. This result confirms the hypothesis of Lindstrom and Magnusson,[97] a part of which was proven by Stulen and De-Luca.[156] A fuller explanation of the mathematical relationships may be found in the Appendix. The work of Brody et al.[24] also showed that during sustained electrical stimulation of the muscle, the rate of change of the CV differed from the rate of change of the MDF and the MNF, implying

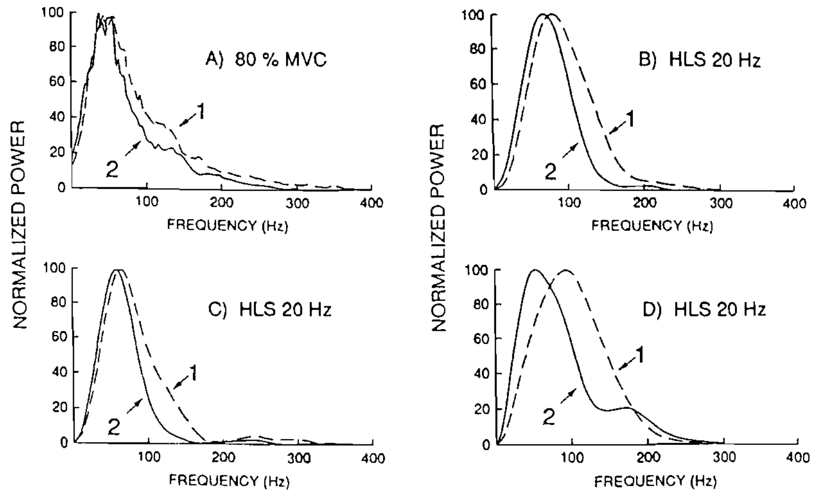

FIGURE 13. Power spectra of voluntary or electrically evoked signals detected from the tibialis anterior of normal subjects with an interelectrode distance of 10 mm. (A) Power spectra of a voluntary myoelectric signal at the beginning (1) and at the end (2) of a 20-s 80% MVC contraction. Each spectrum is the average of two spectra computed on two subsequent 1-s epochs. The resulting spectrum is smoothed by a 20-point moving average filter. Change of shape due to energy reduction in the high-frequency portion of the spectrum is evident. CV shows negligible changes during this contraction and MDF shows normalized changes greater than those of MNF and CV. (B, C, D) Power spectra of the electrically evoked myoelectric signals during the 1st (1) and the 19th second (2) of a 20-s contraction with supramaximal stimulation at 20 Hz. No smoothing filter is applied. (B) The spectrum shows compression without shape change. MNF and MDF show an equal percent decrease. This behavior is relatively common. (C) The spectrum shows compression with shape change. The percent decrease of MNF is greater than that of MDF. This behavior is relatively rare. (D) The spectrum shows compression with shape change. The percent decrease of MNF is smaller than that of MDF. This behavior is common. In order to show shape changes more clearly, all spectra are normalized with respect to their maximum value. Such value is always higher at the end of the contraction because of the amplitude scaling due to compression (see the Appendix for mathematical details).

that factors other than the extracellular pH affect the CV, MDF, and MNF during sustained contractions. These additional factors may be classified into two groups: those contributing to additional spectral compression without affecting the shape of the spectrum, and those causing a change in the spectrum shape. A scaling in space of the MUAP (or the M-wave) belongs to the first group of factors. Possible candidates for the second group of factors are recruitment or derecruitment of motor units during the contraction, a change in the muscle fiber action potential shape, and a nonuniform decrease in CV with consequent spatiotemporal scatter of the depolarization zones.

The increase of the length of the depolarization zone during a sustained contraction has been discussed by Dimitrov,[42] Dimitrova,[43] Gydikov et al.[68,70] and Kostov et al.[87] in a number of papers in which the methodology is not well described. The normal length of the depolarization zones of the fibers of the voluntarily contracting human biceps was reported by these authors to be in the range of 18.36 ± 0.48 mm. During electrical stimulation, normal values were reported in the range of 30.5 ± 1.57 mm, increasing to 37.0 ± 1.2 mm "after fatigue".[70] A model that illuminates the effect of CV, duration, and asymmetry of the action potential of an infinitely long, unmyelinated nerve fiber on the

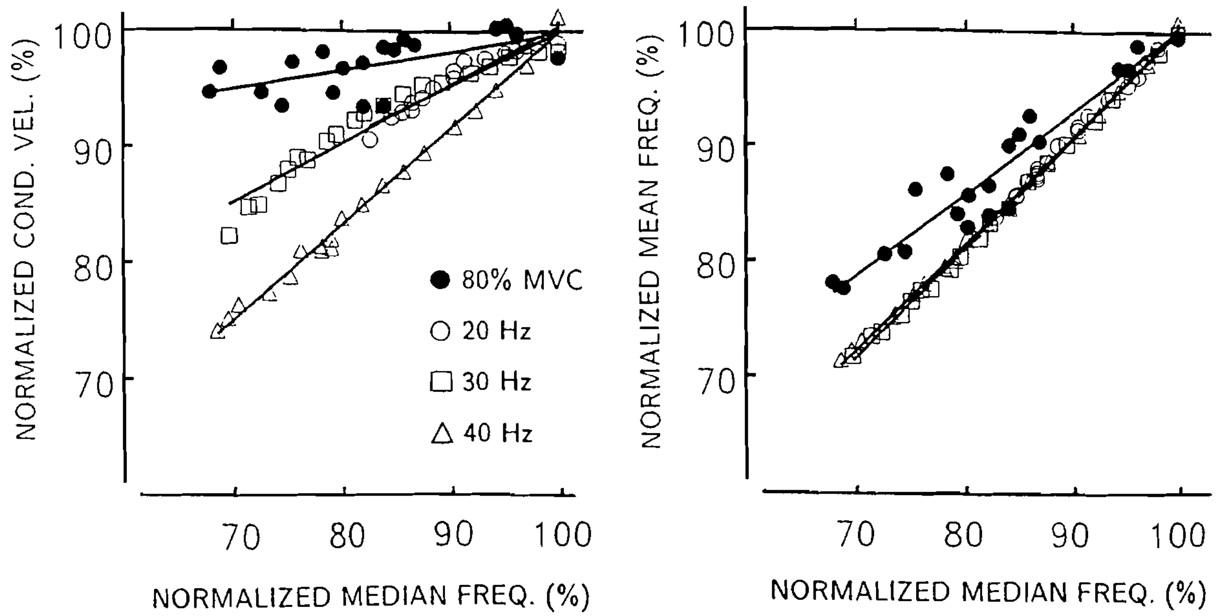

FIGURE 14. Normalized values of CV vs. MDF and of MNF vs. MDF during a voluntary contraction (80% MVC) and during three electrically evoked contractions with supramaximal stimulation at 20, 30, and 40 Hz of a normal tibialis anterior muscle. Contraction duration was 20 s. The regression coefficient of CV vs. MDF is less than unity and is particularly low during the voluntary contraction, indicating that MDF is affected by factors other than CV. The regression coefficient of MNF vs. MDF is near unity during any of the three electrically evoked contractions, suggesting spectral compression, while it is less than unity during the voluntary contraction, indicating change of spectral shape (increase of skewness) during the contraction. The point (100, 100) represents the beginning of the contraction.

extracellular signal PSD has been developed by Lateva.[94] This work clarifies the relationship between depth, CV, and length of the source and the surface signal power spectrum.

It is anticipated that future work on the analysis of the shape of the M-wave and of its change during a sustained contraction may provide some additional insight into the role of these factors and into the information that the M-wave carries about them.

B. Relationship among Spectral Variables, Conduction Velocity, and Number of Stimulation Pulses

Figures 15 and 16 show results obtained from the tibialis anterior of the two normal subjects during supramaximal stimulation of the main motor point at 20, 25, 30, 35, and 40 Hz. Normalized values of MDF and CV are plotted vs. either time or number of pulses for each stimulation frequency. The data in Figure 15 show that MDF and CV are more closely dependent on the number of stimuli rather than on their frequency. Marsden et al.[101] observed a similar behavior for muscle force and stated that, for stimulation frequencies above 20 Hz, the force decrement is a function of the number of pulses delivered rather than their frequency. Figure 16 presents data from a different subject. In this case, greater changes of MDF and CV occur and their relationship with the number of pulses is weaker than in the previous case. It may be speculated that these two subjects had different rates of removal of metabolites (different blood flow) or that their CV and MDF were differently affected by metabolite concentration or ionic shifts. In either case, a different behavior of these two tibialis anterior muscles is evident. One may speculate that for each stimulus applied to a muscle, a fixed quantum of metabolites would be generated. If this were indeed the case, under ischemic conditions, changes of CV, MDF, and MNF would be related to the number of applied pulses rather than to their frequency. Although further research is needed to provide greater insight into the factors described in Figure 11, it is evident that electrical stimulation techniques and M-wave processing

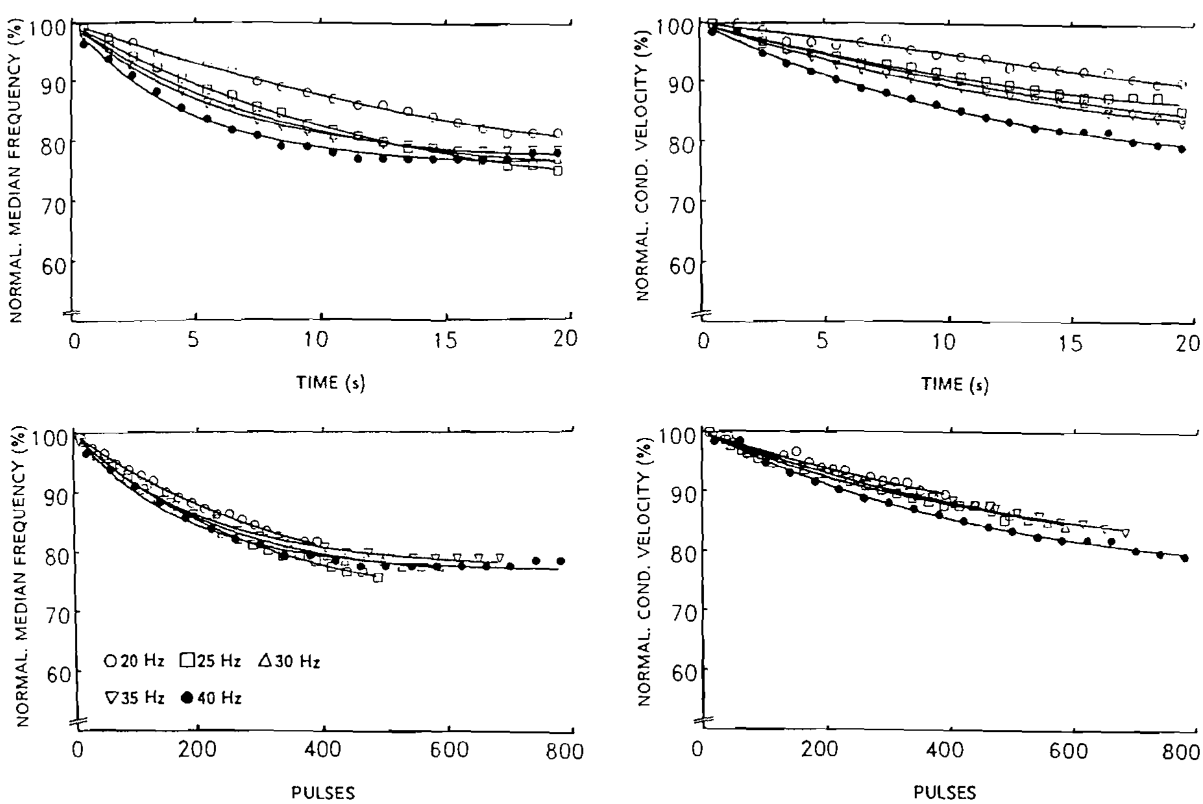

FIGURE 15. Time course of normalized MDF and CV vs. time and vs. the number of applied stimuli during supramaximal electrical stimulation of a normal tibialis anterior at 20, 25, 30, 35, and 40 Hz. Values are normalized with respect to the intercept of the regression curve. Compare with data obtained from a different subject and shown in Figure 16. Linear or exponential regressions are used.

techniques may play an important role in noninvasive muscle characterization.

VIII. ORDER OF RECRUITMENT OF MOTOR UNITS DURING ELECTRICAL STIMULATION

A. Surface Stimulation

It is generally accepted that during a voluntary muscle contraction, the recruitment of motor units progresses from small (mostly slow twitch) to large (mostly fast twitch) units. It has been shown that muscle fibers of larger motor units have a higher CV than those of smaller units and that CV is a "size principle parameter"[6] that reflects recruitment order and increases with increasing level of voluntary contraction.[7,26,82] Data describing the behavior of CV and spectral variables of the ME signal during electrical stimulation are not as abundant as those relating to voluntary contractions.[28,85,124,125] It is generally accepted that with direct nerve stimulation by means of implanted electrodes, the order of recruitment of motor units with increasing stimulus amplitude is the opposite of that occurring during voluntary recruitment;[62,63,127,147–149] however, Brown et al.[27] and Bergmans[16] separately found that when graded electrical stimulation was applied to the median or ulnar nerve via surface electrodes, the first units recruited had the smallest M-waves and the longest latencies, suggesting an order of recruitment similar to the physiological order.

More recently, Knaflitz et al.[85] reported a variable order of recruitment in motor point stimulation of the human tibialis anterior. The authors' work suggested that three factors may play a role in determining the order of recruitment (as indicated by muscle fiber CV changes) during

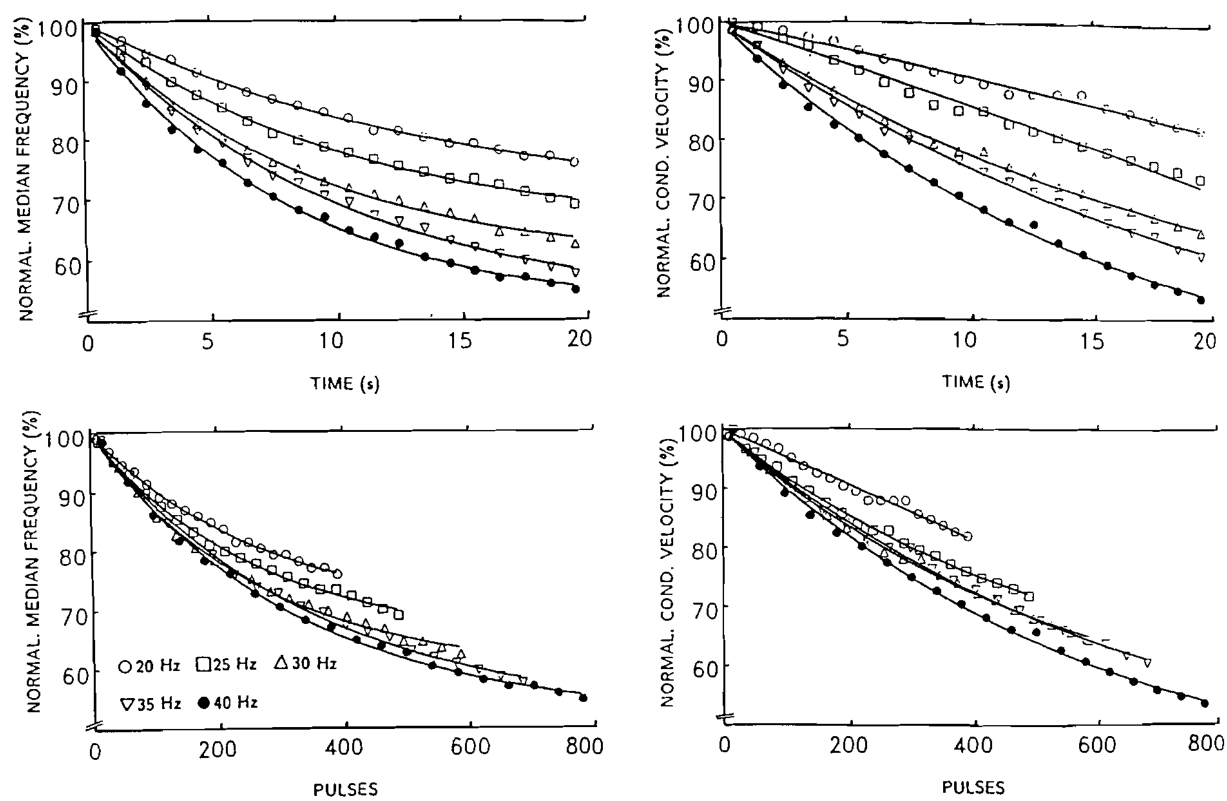

FIGURE 16. Time course of normalized MDF and CV vs. time and vs. the number of applied stimuli during supramaximal electrical stimulation of a normal tibialis anterior at 20, 25, 30, 35, and 40 Hz. Values are normalized with respect to the intercept of the regression curve. Compare with data obtained from a different subject and shown in Figure 15. Linear or exponential regressions are used.

surface electrical stimulation of muscle motor points:

1. The size of the axon, which is known to be related to excitability threshold, to the size of the motor unit, and to the average size of its muscle fibers.
2. The size of the motoneuron branches, whose diameter is related to their excitability threshold.
3. The location and the orientation of the motoneuron branches in the current field.

Apparently factors (2) and (3) play an important, if not dominant, role since recruitment order with increasing surface stimulation intensity (although not predictable *a priori*) appears to mimic voluntary recruitment order in most cases. This behavior might be specific to muscles that, like the tibialis anterior, seem to have progressively larger fibers in progressively deeper regions.[75] In general, axonal diameter (i.e., the motoneuron electrical excitability threshold) is not a critical factor in determining motor unit recruitment order during surface stimulation of a muscle motor point. It is suggested that terminal branches of large motoneurons could be either smaller or more deeply located than those of smaller motoneurons and, therefore, may be excited only at higher current levels. Such a hypothesis would explain the finding of similar recruitment order during voluntary and electrically evoked contractions observed in 23 out of 32 experiments reported by Knaflitz et al., and indicated in Figure 17.

B. Direct Nerve Stimulation

Direct nerve stimulation may be obtained by means of electrodes inserted into or wrapped around a motor nerve trunk. It is known that the progressive increase of stimulus amplitude or duration recruits progressively more motoneurons

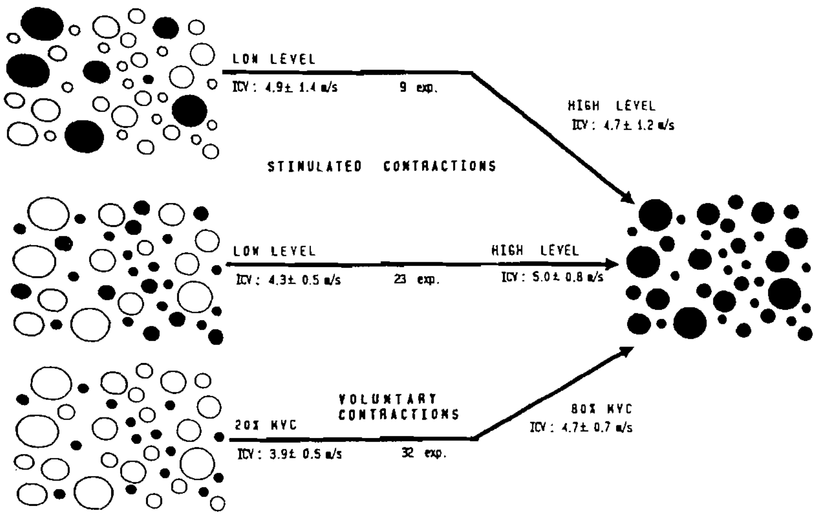

FIGURE 17. Schematic representation of recruitment order during voluntary and electrically evoked contractions.[85] When the voluntary contraction level is increased from 20 to 80% MVC, CV increases in all 32 experiments performed. When stimulation current is increased from a "low level" (corresponding to an M-wave about 30% of the maximal) to a "high level" (corresponding to the maximal M-wave), initial conduction velocity (ICV) increases in 23 experiments and decreases in 9. Since ICV values can be associated to fiber size,[6] these data allow inference on recruitment order.

in an order that is macroscopically opposite with respect to that of the size principle[30,62,63,147,160] because the strength duration curves of the smallest nerve fibers are above those of the largest fibers (see Figure 18A). However, specific modalities of electrical stimulation have been found to produce blocking or selective activation of nerve fibers. Particular stimuli shapes,[1,52,53] polarizing currents,[5] or high frequency stimuli[13,22,152,161] have been studied. The latter technique is particularly interesting and promising because it has been reported to achieve orderly recruitment of motor units by using a combination of electrical stimulations at two separate sites on a nerve. A schematic representation of the system is shown in Figure 18B and C. A set of electrodes applies supramaximal pulses at the desired rate (rate stimulation), while a second set of electrodes, positioned distally with respect to the first, applies a train of monopolar rectangular pulses (600 pulses per second; 40 to 100 μs pulse-width) that produce blockage of muscular activation. As the amplitude of the blocking stimulus is reduced, the nerve fibers escape from the block in order of increasing size, and the respective motor units may therefore be activated by the "rate stimulus" pulses. Recruitment and de-recruitment of motor units (macroscopically according to the size principle) may then be obtained by decreasing the amplitude of the blocking stimulus from the total block to zero.

Application of this technique on the sciatic nerve of cats showed that orderly recruitment of motor units appeared to produce an increase in CV and MDF of the electrically evoked myoelectric signals.[151] This agrees with the previous observations of Broman et al.[26] and of Knaflitz et al.[85] in the human tibialis anterior muscle. The technique has also been used to confirm that the relationship between the amplitude of the myoelectric signal and force output of a muscle is a function of the recruitment/firing rate strategy employed by the muscles, as was first proposed by Lawrence and DeLuca.[95]

C. Motor Unit Counting

Since a muscle consists of a finite number of motor units, each being activated in a all-or-none fashion in response to an electrical pulse, it follows that a slowly increasing electrical stim-

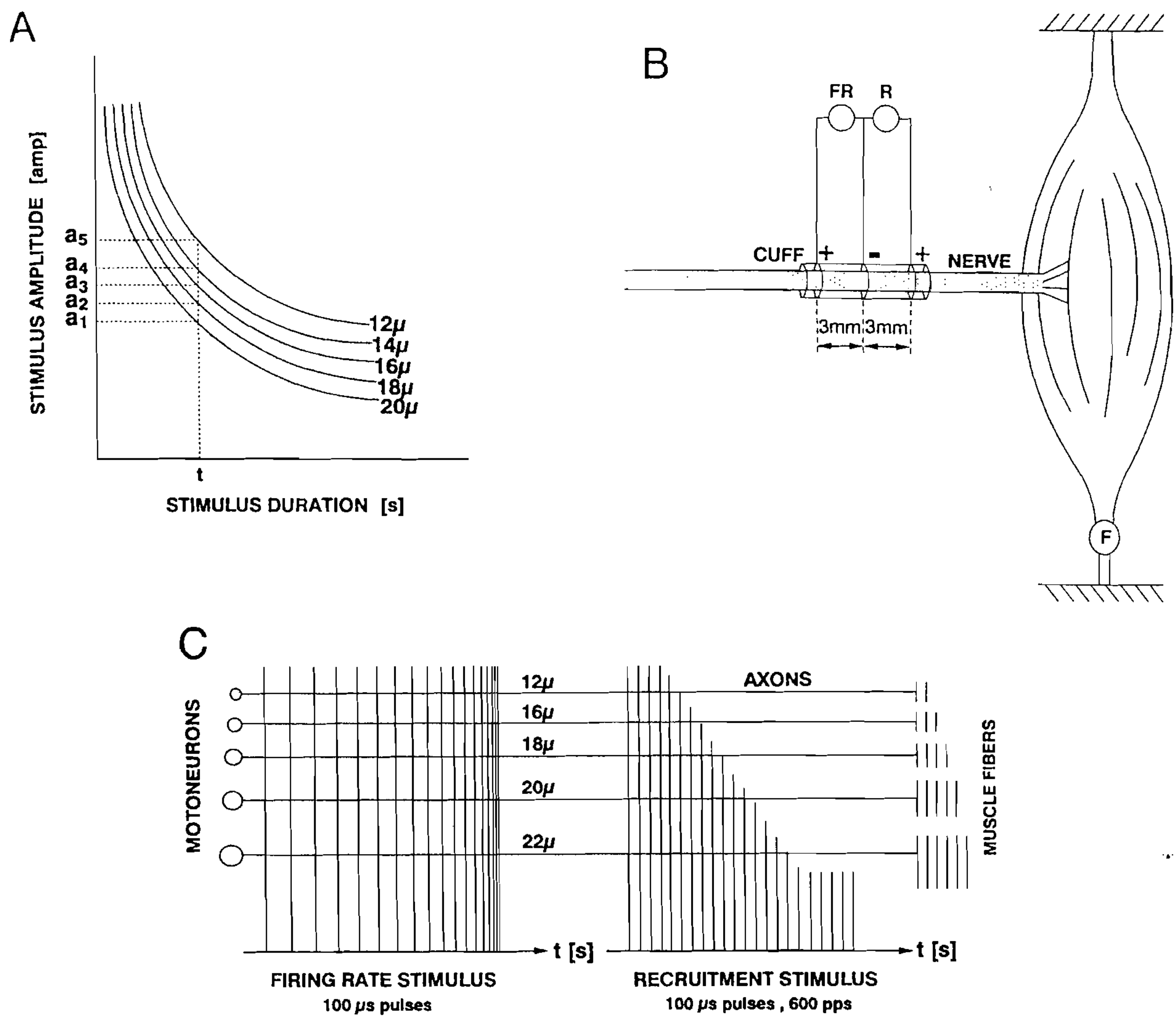

FIGURE 18. (A) Schematic diagram of the strength-duration curves of nerve fibers of different sizes.[152] (B) Schematic representation of the tripolar cuff electrode mounted on the nerve-muscle preparation. FR: firing rate stimulus; R: blocking stimulus. F: force transducer. Progressive reduction of the R stimulus allows nerve fibers of increasing size to escape the block, allowing recruitment in order of increasing size of motoneuron axons and motor units. (C) Schematic representation of the recruitment of nerve fibers in order of increasing size by progressive reduction of the blocking high frequency stimulus. Increase of muscle contraction strength is obtained by increasing the firing frequency of the recruited motor units and by simultaneous recruitment in order of increasing motor unit size.[13,152]

ulus would lead to an increase of the evoked response in discrete increments. Each elementary increment would result from the excitation of an additional motor unit. In 1971 and 1973, McComas et al.[104,105] reported that they had been able to count between 121 and 412 motor units in the extensor digitorum brevis of the feet of 41 normal human subjects, and used their technique to demonstrate motor unit loss in pathological situations. Despite its simplicity, the technique has not achieved widespread use because of a number of limitations inherent in the methodology and in its application; however, with the availability of computer-controlled equipment, the method was revived in 1991.[106]

IX. MYOELECTRIC MANIFESTATIONS OF FATIGUE IN ELECTRICALLY STIMULATED MUSCLES

Myoelectric signal variables show time-dependent changes during constant force contractions. These changes reflect ongoing physiological modification of the muscle fibers, leading to nonstationarity of the signal (see Section VI), and are referred to as myoelectric manifestations of muscle fatigue.[14,39]

It has been known for approximately two decades that time-dependent modifications in the myoelectric signal are the result of time-dependent modifications in the MUAPs, but perhaps the most revealing study on this topic is that of Sandercock et al.[144] who studied the changes in individual MUAP of electrically activated motor units in the medial gastrocnemius of the cat. Intermittent stimulation (0.3 s on and 0.7 s off) at 40 Hz for 120 s of a fast-twitch motor unit led to the results shown in Figure 19A. Continuous stimulation at 80 Hz led to the results shown in Figure 19B. The extracellular potential of individual muscle fibers was also detected and showed a rapid decrease followed by a lack of excitation. A number of conclusions may be drawn from Figure 19:

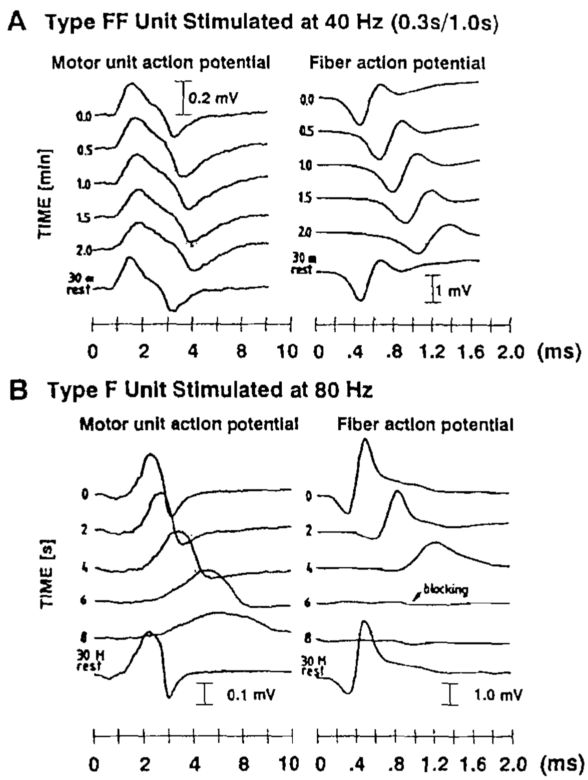

FIGURE 19. (A) Example of MUAP and fiber action potential from a type FF (fast fatigable) motor unit from the medial gastrocnemius of a cat during intermittent stimulation at 40 Hz (0.3 s of stimulation delivered every second) for 2 min and after a 30-min recovery period. (B) Example of MUAP and fiber action potential from a type F (fast) motor unit from the medial gastrocnemius of a cat during continuous stimulation at 80 Hz for 8 s and after a 30-min recovery period. (From Sandercock, T. G. et al., *J. Appl. Physiol.*, 58(4), 1073, 1985. With permission.)

1. Intermittent electrical stimulation at 40 Hz (duty cycle = 1/3) allows a motor unit of fast-twitch fibers to respond for minutes, while under continuous stimulation at 80 Hz the MUAP vanishes after a few seconds. This behavior could be interpreted in terms of metabolite production and removal dynamics or in terms of ionic shifts taking place with some dynamics that allow restoration of membrane properties between intermittent contractions while it leads to cumulative effects under continuous higher frequency stimulation.
2. During intermittent stimulation, some fibers of the motor unit show an increase of latency and of response duration on the order of 30 to 40%, indicating a change of CV and, possibly, additional factors. However, the individual MUAP shows a smaller percentage of change, suggesting that the changes of single fiber variables may be very nonuniform and, therefore, the decrease of average CV of the motor unit fibers may be accompanied by an increase of CV standard deviation, leading to a low-pass filtering effect.[97]
3. Continuous high frequency (80 Hz) stimulation of a fast-twitch type motor unit rapidly leads to a decrease in amplitude and to the disappearance of single fiber action potentials. This observation supports the hypothesis that both the amplitude and shape of a MUAP are altered during sustained stimulated contractions.

Other electrical manifestations of muscle fatigue at the single fiber level have been reported by Hanson,[73] who measured *in vitro* the single fiber action potentials in the extensor muscle of the antebrachium and in the soleus of rats. Hanson showed that after repetitive stimulation, the resting membrane potential rises toward zero, the amplitude of the action potential decreases, and its duration increases. Such changes were much more marked in the mostly fast fibers of the extensors than in the mostly slow fibers of the soleus. Contraction time and half-relaxation time were significantly shorter in the extensor muscle than in the soleus. Krjnevic and Miledy[90] found that only a few muscle fibers could conduct action potentials for longer than 1 min when stimulated continuously at 50 Hz.

The role of the ionic concentrations (H^+, K^+) across the muscle fiber membrane in determining the amplitude and the duration of the action potentials has been studied by many authors[2,80,127] in animal muscles. In particular, Jones[80] studied the action potential of single fibers *in situ* (human abductor pollicis) and *in vitro* (rat diaphragm) and observed that the reduction of amplitude and increase of duration of action potential observed in humans following electrical stimulation could be mimicked in the rat diaphragm by changing the extracellular concentration of K^+ from 5 to 10 m*M*/l, as indicated in Figure 20. The same author also observed a change in the excitation threshold of motor units during fatiguing contractions, indicating that the changes in myoelectric signals during a sustained electrically evoked contraction may be due to the combined effect of a reduction of the number of active motor units and a reduction of amplitude and an increase of duration of the MUAP of the individual active motor units. Brody et al.[24] have recently shown that a change in the extracellular pH also causes a change in the same direction in the CV of the muscle fibers of the rat diaphragm. The change in the CV causes a scaling of the MUAP in the time domain, but does not cause a change in the fundamental shape of the MUAP. This observation is important because it is known that during sustained contractions the pH of the extracellular fluid decreases. Thus, we know that a causal relationship exists between the pH in the extracellular fluid inside the muscle and the myoelectric signal outside the muscle.

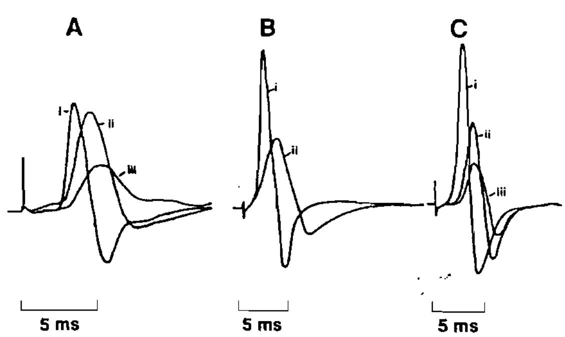

FIGURE 20. Slowing of action potential waveforms in muscle preparations *in situ* and *in vitro*. (A) Action potentials recorded from the human adductor pollicis after 2 s (i), 20 s (ii), and 40 s (iii) of stimulation of the ulnar nerve at 50 Hz. (B) Action potential of isolated and curarized strip of rat diaphragm after 1 s (i) and 10 s (ii) of stimulation at 50 Hz. (C) Action potentials from an isolated rat diaphragm preparation in response to single shocks at intervals while the K^+ concentration of the medium was increased from 5 m*M*/l (i) to 10 m*M*/l (iii). (From Jones, D. A., in *Human Muscle Fatigue: Physiological Mechanisms,* Ciba Foundation Symposium, Pitman Medical, London, 1982, 178. With permission.)

Some of these findings have been verified to apply to human muscles as well. For example, Moritani et al.[124] reported an amplitude reduction and a "slowing" of the electrically evoked potential that was much greater in the gastrocnemius than in the soleus of normal men, reflecting the different fiber type constituency of the two muscles.

The body of evidence presented above indicates that during a stimulated contraction, the electrically evoked myoelectric signal undergoes changes in amplitude, duration, and shape due to a number of factors, including variations of the active motor unit pool. These results also suggest that fast-twitch motor units are the first to be de-recruited. Furthermore, the literature contains strong indications that the histochemical, mechanical, and electrophysiological properties of muscle fibers are interrelated and, therefore, electrophysiological data may be expected to provide information on muscle fiber constituency and mechanical muscle performance. However, such relationships must be considered with caution, as indicated by the results of Merletti et al.,[114] who compared myoelectric manifestations of fatigue between young adults and elderly subjects during sustained isometric voluntary or electrically evoked contractions of the tibialis anterior. During voluntary contractions at 80% MVC sustained for 20 s, elderly subjects showed decrements of CV, MDF, and MNF that were significantly smaller than those of young adults, suggesting a possibly higher percentage of type I fibers with respect to the young adults.

However, during supramaximal stimulation at 40 Hz the decrements were similar in the two groups, suggesting that highly fatiguing electrically evoked contractions might mask, rather than outline, differences related to muscle fiber constituency.

A. Sustained Contractions

The changes of amplitude, duration, and shape of the MUAP during sustained voluntary or electrically evoked contractions cause the myoelectric signal to be nonstationary. Different types of nonstationarity may be identified and associated with different physiological factors. The best known type of nonstationary behavior is a progressive time scaling of the signal in the time domain and a corresponding inverse scaling in the frequency domain (see Appendix). It is therefore a *frequency compression* and not a *frequency shift*, as it is often improperly referred to in the literature, especially when the PSD function is displayed vs. logarithmic frequency scales. Amplitude parameters and the autocorrelation function are also affected by this phenomenon (see Appendix). Other types of nonstationarity imply a change of spectral shape, as well as a change in signal shape in the time domain.

The time course of torque and myoelectric signal variables during isometric, electrically evoked contractions sustained for 20 s has been investigated by Knaflitz et al.[85] and Merletti et al.,[112] who recently reported the following observations on the human tibialis anterior (see Figure 21):

1. Supramaximal electrical activation of a motor point elicits ankle joint torques in the range of 7 to 32% MVC,[85] indicating that only a portion of the muscle is activated while the entire anterior compartment is activated by voluntary contraction. This value is lower than the 40% MVC reported by Milner and Quambury[120] for the quadriceps, probably because of the more selective technique used by Knaflitz et al.[85]
2. Muscle force usually shows a slight increase during a 20-s electrically evoked contraction, indicating a lengthening of the twitch response which, for a fixed firing rate, results in increased torque. In a few cases, force slightly decreased, suggesting a dominant effect of mechanical fatigue (twitch decrement) over twitch lengthening.
3. Estimates of myoelectric signal variables show less variability during stimulated than during voluntary contractions (indicated in Figure 21).
4. The normalized decrement (or percentage of change) of spectral variables is greater than that of CV during either voluntary or electrically evoked contractions, indicating that factors other than CV affect the myoelectric PSD function (indicated in Figure 21).
5. The decrement of CV, MDF, and MNF appears to be more closely related to the number of pulses applied to the muscle rather than to their frequency, suggesting a relationship between the number of pulses and the amount of metabolites produced (see Figures 15 and 16).
6. The greater changes in MNF and MDF with respect to those in the CV suggest a progressive increase of the length of the spatial potential distribution on the skin. This increase would not affect CV but would affect MNF and MDF.

During sustained stimulated contractions, ARV and RMS show a dome-shaped curve due to the initial widening and subsequent amplitude reduction of the M-wave.[18] This may be attributed to a change in CV and in action potential amplitude, reflecting changes in extracellular Na^+ and pH[24,80] and, eventually, the lack of excitation of individual fibers or of entire motor units.[144]

The above observations are mostly qualitative but clearly indicate that a "global" fatigue index cannot be easily defined since different mechanical and electrophysiological variables behave very differently during a fatiguing contraction. A quantitative approach to the issue of fatigue requires the definition of fatigue indices suitable for describing the time course of individual variables such as force or torque, MDF,

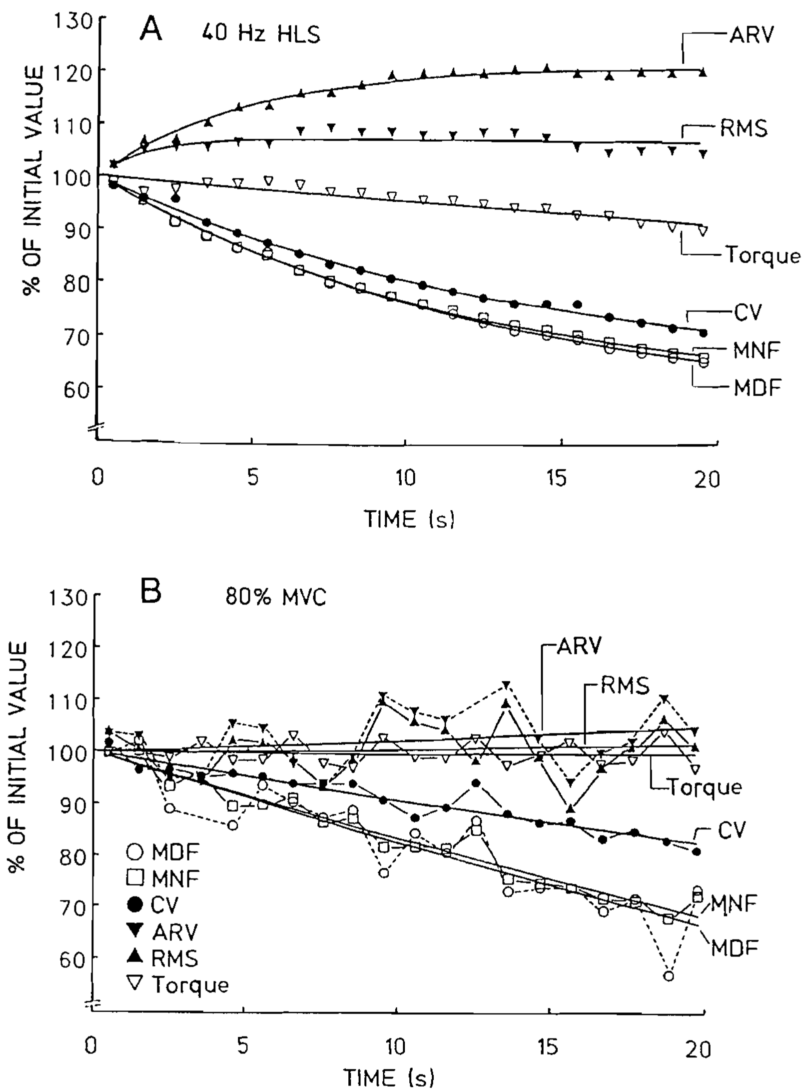

FIGURE 21. Example of normalized values (normalization with respect to the intercept of the regression curve or line) of ARV, RMS, torque, CV, MNF, and MDF during a 40-Hz supramaximal electrically evoked contraction (A), and a 80% MVC (B) from the tibialis anterior of the same healthy subject. Much smaller fluctuations of the estimates are evident during the stimulated contractions. The similar decrements of MDF and MNF indicate spectral compression without significant spectral shape changes (see Appendix). The increase of the ARV is greater than that of the RMS value, as theoretically predicted, and is more evident during the stimulated contraction. Force fluctuations are virtually absent during the stimulated contraction, and mechanical fatigue is minimal in both contractions. The smaller rate of change of CV with respect to either MDF or MNF is more evident in the voluntary contraction. HLS = high-level (supramaximal) stimulation.

CV, etc. To reach this goal, it would be highly desirable to meet the following conditions:

1. The number and (possibly) the firing rate of the active motor units should remain constant during the contraction so that a fatigue index would describe the behavior of that specific motor unit population at a specific firing rate.
2. The estimates of the variable of interest must be affected by a small standard deviation so that the time course of the variable can

be defined accurately and small changes in time may be resolved.

3. A quantitative, unambiguous fatigue index describing the time evolution of the specific variable should be defined. This index should be applicable to either voluntary or electrically evoked contractions and to time patterns that show either linear or curvilinear behavior of myoelectric signal variables.

Sustained, isometric, electrically evoked contractions provide an experimental paradigm that closely meets conditions (1) and (2), as indicated in Figure 21. An index that satisfies condition (3) was recently proposed by Merletti et al.[113] and is defined in Figure 22. This index may be computed either as an attribute of the contraction or as a function of time; it is regression free, dimensionless, normalized, and not very sensitive to local fluctuations. It varies between 0 and 1 for decreasing patterns and is negative for increasing patterns. This index is highly sensitive to the proper choice of the reference value y_r, a property that makes it more suitable for electrically evoked contractions that show smaller variances of the variables than voluntary contractions, as indicated in Figure 21.

The evidence reported above indicates that, during an electrically evoked contraction, myoelectric or mechanical manifestations of muscle fatigue can be described more rigorously than is allowed by voluntary contractions. In addition, electrical stimulation may induce a faster and greater level of muscle fatigue than occurs during voluntary activation. These conclusions must be taken with caution. For example, they do not necessarily imply that stimulation may provide a better understanding of phenomena taking place during voluntary contractions. Furthermore, it must be emphasized that the electrically stimulated muscle is operating under conditions very different from those existing under voluntary control, and if motor point stimulation is used, repeatability of measurements is limited by the sensitivity of the activated muscle portion to electrode location. Unfortunately, no one has yet reported repeatability assessments for either motor point or nerve trunk stimulation.

B. Intermittent Contractions

Sustained isometric contractions are appropriate for muscle testing purposes because they

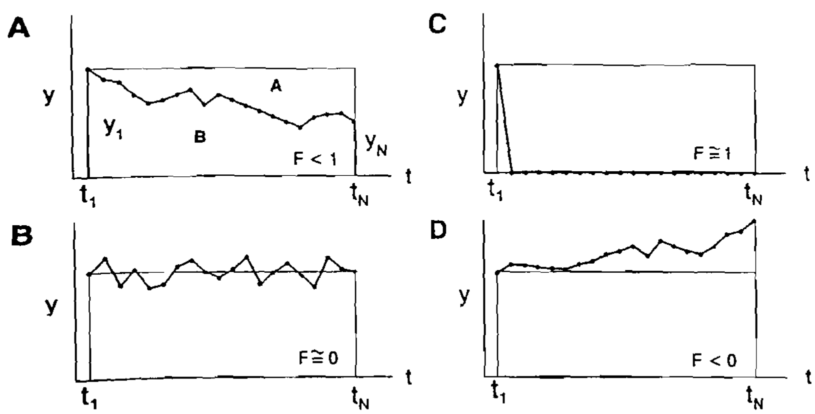

FIGURE 22. Definition of the area ratio index F as:

$$F = 1 - \frac{B}{A+B} = 1 - \frac{B}{y_r t_c} = 1 - \frac{1}{2(N-1)y_r} \sum_{i=1}^{N-1} (y_i + y_{i+1})$$

where y may be torque or any myoelectric signal variable (CV, MNF, ARV, etc.). Examples of data showing $F < 1, F \sim 0, F \sim 1, F < 0$. The reference value y_r is taken as $y_r = y_1$. The area ratio may be presented as absolute value F or relative (%) value 100 F.

provide easily controllable experimental conditions. Such contractions are not common in everyday life; intermittent anisometric contractions are far more common. Intermittent contractions induce dynamic changes of muscle variables at the turn-on and turn-off time of each contraction. For example, this is the case during FES applications. Different muscle variables, either electrical or mechanical, show different dynamic behavior and very different time constants in response to a rising or falling step of muscle activation. This fact is clearly indicated by the work of Milner-Brown and Miller,[121] who studied the myoelectric signal and the twitch contraction of the human first dorsal interosseus, abductor pollicis, and tibialis anterior in response to single stimuli applied to the ulnar or peroneal nerve after a 100% MVC isometric contraction sustained for 1 or 2 min. They found a decrease in amplitude and an increase in duration in the electric response associated to a decrease of twitch amplitude. The recovery to normal values of the electrical response required 45 to 240 s after 1 min of 100% MVC and 2 to 10 min after 2 min of 100% MVC. Recovery of twitch amplitude was much slower, indicating a difference in the dynamics of electrical and mechanical variables.

Muscle blood flow undergoes changes during intermittent contractions as does the removal of metabolites. Therefore, the concentration of metabolites and the amount of ionic concentration shifts are functions of the duty cycle of a periodic intermittent contraction and so are the muscle variables, as indicated by the work of Duchateau et al.[44,45] and of Hainaut and Duchateau.[71] These authors compared electrically evoked contractions of the adductor pollicis (supramaximal stimulation at 30 Hz) sustained for 60 s with a sequence of 60 intermittent tetanic contractions of 1 s each with 1-s intervals in between. Their results are shown in Figures 23 and 24, and clearly show the different muscle performances in response to the two experimental paradigms. The 1-s contractions of the intermittent protocol might have been too short to assess the M-wave parameters because of the transient due to muscle movement underneath the electrodes (see Figure 3). Despite this possible flaw, this work shows that myoelectric signal changes are not closely related to mechanical changes and may not be directly used to predict or describe them in intermittent contractions unless the dynamics of the different variables are taken into account.

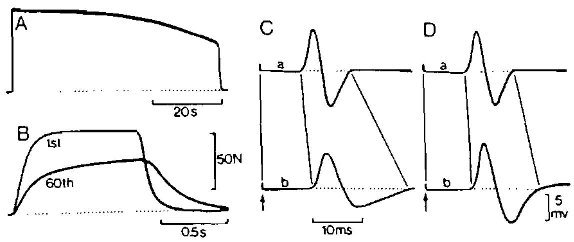

FIGURE 23. Comparison of tetanic force and M-wave changes during a 60-s sustained contraction and during a series of 60 1-s contractions spaced by 1-s intervals in the adductor pollicis of a human subject. Supramaximal stimulation of the ulnar nerve at 30 Hz. (A) During the sustained contraction force decrement is 42%. (B) During the intermittent contraction force decrement is 38%. (C) M-wave recorded after 1 s (a) and after 60 s (b) of sustained contraction. The arrow indicates the stimulus. (D) M-wave recorded during the first (a) and last (b) 1 s contraction. The arrow indicates the stimulus. (From Hainaut, K. and Duchateau, J., *Muscle Nerve,* 12, 660, 1989. With permission.)

The work of Zijdewind et al.[162] provides further evidence of "independence" between M-wave parameters and force in intermittent contractions. However, these authors used 30-Hz supramaximal stimulation of the ulnar nerve with 0.33 s on-time and 0.67 s off-time, thus applying bursts of only 10 pulses. Such a pulse train may be too short to allow for the stabilization of the M-wave and exhaustion of the transient due to muscle movement, as indicated in Figure 3. Recovery after fatigue was observed using either single pulses or short bursts (0.33 s) at 30 Hz, without considering the possible effects of movement artifacts.

Stokes et al.[155] studied the abductor pollicis by supramaximal stimulation of the ulnar nerve with a protocol of step-like frequency increase from 1 to 100 Hz within a single train of pulses lasting 17 s. At 50 Hz, and more so at 100 Hz, the M-waves interfere with each other because the interstimulus interval is shorter than the M-wave duration, and measurements of M-wave parameters are flawed. In addition, any measurement of electrical variables during stimulation at 100 Hz would be affected by the rapid fatigue induced by the previous stimulation at 50 Hz. The protocol used by Garner et al.[58] seems to be

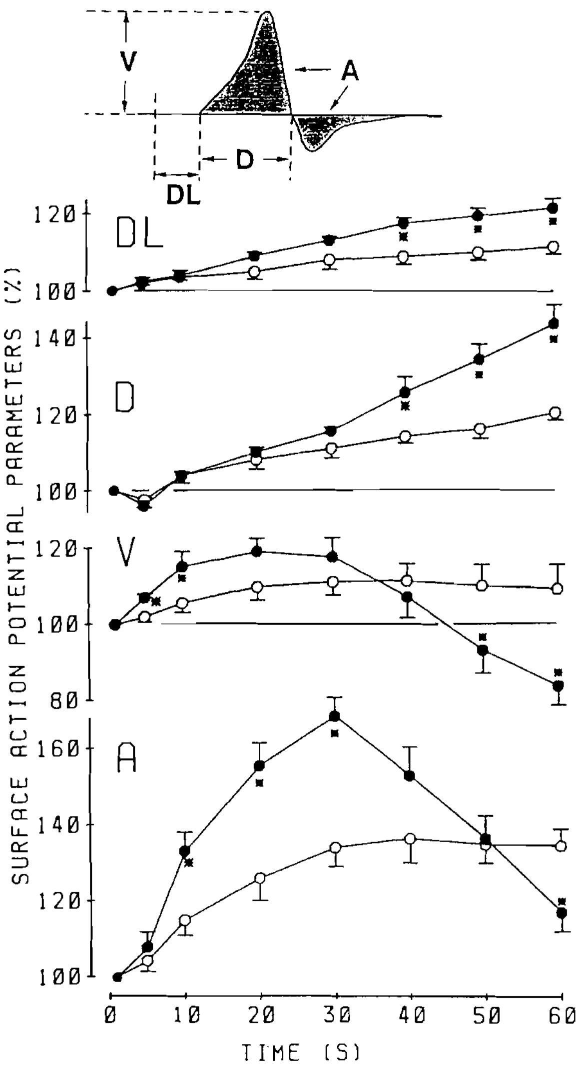

FIGURE 24. Adductor pollicis of the same subject as Figure 23. Comparison of the time course of M-wave variables during a 60-s sustained contraction (•) and in a series of 60 1-s contractions spaced by 1 s intervals (o). Supramaximal stimulation of the ulnar nerve at 30 Hz. Changes are expressed as percent of control values measured from the 30th response. Values are means ± standard error of the mean with N = 5. Stars indicate differences significant at the 0.05 level. DL: latency between stimulus and M-wave onset; D: duration of the first M-wave phase; V: amplitude of the first M-wave phase; A: area of the M-wave. (From Hainaut, K. and Duchateau, J., *Muscle Nerve,* 12, 660, 1989. With permission.)

more useful. They stimulated the peroneal nerve for 3 s on and 2 s off, detected M-waves from the TA muscle and showed that during 3 min of this intermittent stimulation the amplitude of the response did not change significantly, while muscle twitch force increased 100% during the first 30 s, then decreased to about 25% of the control value during the remaining 150 s. After stimulation was interrupted, periodic tests indicated a stable M-wave amplitude and a decreasing force for the next 50 min. A number of previous papers (see References 31, 57, and 77) provide additional evidence of very different behavior in myoelectric signal variables and force recovery during intermittent contractions, indicating that the membrane phenomena, responsible for myoelectric signal generation, have shorter recovery time constants than the contractile phenomena responsible for force production.

This body of evidence shows that the myoelectric signal variables may provide rather misleading representations of muscle force during intermittent contractions or during recovery from fatigue since a given value of a variable may correspond to very different force levels, depending on the previous history of the contraction. Proper force information might be recovered only through the use of appropriate models that account for the dynamics of the different variables and of the force. A variety of protocols have been reported for investigating the electrically evoked myoelectric signal force relationship and some of these protocols are not useful. In addition, attention has been focused almost exclusively on signal amplitude variables and not on CV or spectral variables, which may provide more useful information and certainly deserve more consideration.

It can be concluded that the results obtained from sustained isometric, constant force contractions cannot be readily extrapolated to intermittent contractions and that additional work is needed to assess how myoelectric signal variables obtained during dynamic or intermittent isometric contractions may be used to monitor or predict mechanical muscle fatigue. Presently, the findings obtained during sustained contractions remain valid only for sustained contractions and should not be extrapolated to other experimental situations.

X. ASSESSMENT OF CROSSTALK BY ELECTRIC STIMULATION

A. Crosstalk Definition and Assessment Techniques

From an electrical point of view, the human body may be thought of as a volume conductor surrounded by a resistive sheath (the skin). The volume conductor behaves as a spatial low-pass filter,[97] the cutoff frequency of which depends on the distance between the signal source and the detection electrode. Consequently, high spatial frequency components of the signals generated relatively far from the detection electrodes are attenuated more than those of signals generated relatively closer. The amount of attenuation due to the tissue filtering effect mainly depends on (1) the relative distance between signal sources and detection electrodes, (2) the spatial frequency content of the signal along the muscle fiber, (3) the geometry of detection electrodes (shape and dimensions of the active surfaces, interelectrode distance), and (4) the structure of the spatial filter (see Figure 2).

In electromyography, crosstalk is defined as the signal generated by a given muscle and detected above or inside a different muscle.[40,116] An important clinical consequence of crosstalk is the likelihood of arriving at an erroneous conclusion of coactivation among different muscles when only one muscle is active. For example, crosstalk may provide an explanation of the curious observations reported by several authors[64,128,131] who described a response in the tibialis anterior concomitant with the H-reflex induced in the soleus and by Hutton et al.[79] who observed the H-reflex recorded over the soleus and the concomitant response of the tibialis anterior induced by stimulation of the posterior tibial nerve in six normal human subjects.

When using indwelling electrodes, the amount of crosstalk in myoelectric signal recordings is generally irrelevant. This is due to the high spatial resolution (small detection volume) of this kind of electrode.[97,139] The situation is totally different when surface electrodes are used. In a number of applications, it is desirable to detect signals generated in a relatively large tissue volume (on the order of cubic centimeters), to obtain a more *global* representation of time and intensity of muscle activation. Among applications requiring global information about muscle activity are muscle fatigue evaluation, gait analysis, and other studies on biomechanics, orthotic and prosthetic control, and biofeedback therapy.

Crosstalk was first identified and described in 1949 by Denny-Brown,[41] who observed that electrical activity may be detected from totally inactive or denervated muscles when a neighboring muscle is intensely activated. More recent reports have come from Gath and Stalberg[59] and Gydikov et al.[69] In 1981, Perry et al.[136] demonstrated that surface myoelectric signals detected above the soleus or gastrocnemius could be expressed as a weighted average of signals coming from the two muscles and from the tibialis posterior, thus clearly illuminating the relevance of crosstalk in surface electromyography. In 1985, Etnyre and Abraham[51] showed that during voluntary contractions of the human tibialis anterior a myoelectric signal could be detected with surface electrodes located over the soleus muscle, while no signals could be detected by means of wires inserted in the same muscle. In 1985, Morrenhof and Abbink[126] measured the amplitude of signals detected by means of surface and wire electrodes, placed above and inside the biceps femoris, the semitendinosus, and the adductor magnus muscles in the human thigh. Myoelectric signals recorded by different pairs of surface electrodes were found to be correlated, and this finding was interpreted by the authors as a sign of volume conduction. It should be emphasized that crosstalk evaluations based on the cross-correlation between signals may be flawed by the intrinsic nonlinearity of the transfer function between the two detection electrode sets, due to the anisotropy and nonhomogeneousness of the interposed tissue.

In 1986, Nielsen et al.[131] and Mangun et al.[100] demonstrated that myoelectric signals could be detected over denervated muscles of cats when a neighboring muscle was activated. Figure 25 shows the surface detected muscle activity induced in the lateral gastrocnemius of cat by stimulation of the dorsal roots at the L7 to S1 level, as well as the myoelectric signal detected over the denervated tibialis anterior. In 1987, De Luca and Merletti[40] suggested a crosstalk assessment

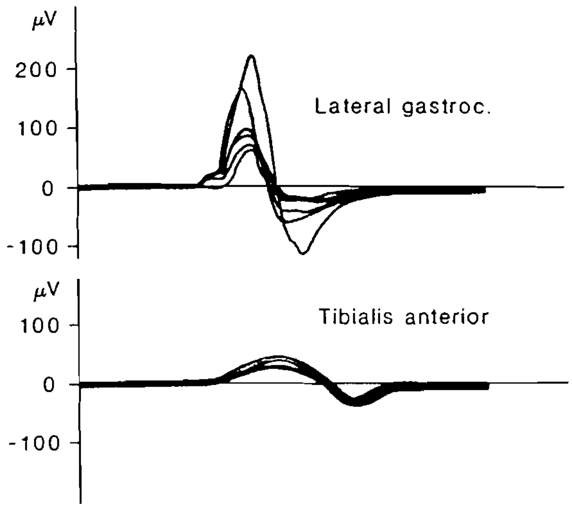

FIGURE 25. Surface-detected reflex activity induced in the lateral gastrocnemius of the cat by stimulation of dorsal roots at L7 to S1 level and signal detected on the denervated tibialis anterior showing volume conduction. (Provided by R. P. Nielsen.)

technique based on electrical stimulation of individual muscles.

B. Assessment of Crosstalk by Electrical Stimulation

The optimal paradigm to quantify crosstalk would be to activate one muscle at a time while measuring signals due to volume conduction on neighboring muscles. Although this task is difficult to perform during voluntary contractions, it can be achieved by stimulation of muscle motor points via surface electrodes, as described by De Luca and Merletti.[40] Crosstalk measurements also require the ability to discriminate between volume-conducted signals generated by muscles near and far from the detection electrode. This goal may be reached by using the multielectrode detection system proposed by Broman et al.[25] (see Figure 2). This detection system provides one SD and two DD signals with different spatial resolution; consequently, when a signal is generated below the detection electrode, it causes SD and DD signals that have approximately the same amplitude. If the signal source is far from the detection electrode, the DD contribution decreases much faster than the SD contribution. Figure 26 shows signals evoked by the stimulation of human vastus lateralis and recorded from the vastus lateralis (A) and from the vastus medialis (B), respectively. An obvious difference exists between SD and DD activity when the signals are collected over the stimulated muscle and when they are due to crosstalk from the vastus lateralis to the vastus medialis.

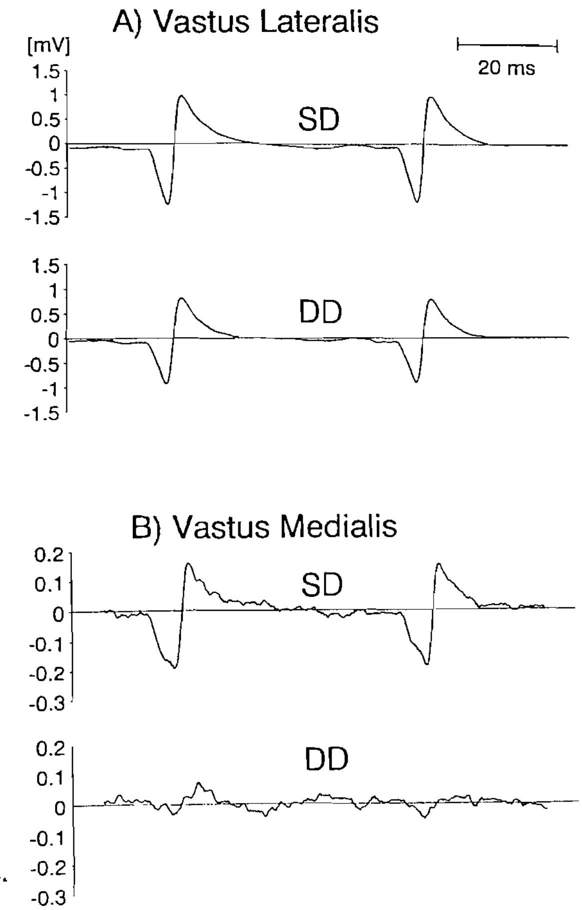

FIGURE 26. Example of SD and DD signals detected above vastus lateralis (A) and vastus medialis (B), respectively, during supramaximal stimulation of the vastus lateralis. The different spatial filtering characteristics of SD and DD detection systems yield DD signals amplitude similar to that of SD signals when the probe is above the stimulated muscle, while the DD signal is negligible when the probe detects SD crosstalk signals.

De Luca and Merletti[40] defined the crosstalk index as the ratio between amplitude parameters of the SD signal detected above the stimulated muscle and those of signals detected on nearby muscles. The combined use of selective stimulation and of the DD technique appears to provide the most convincing paradigm thus far presented for crosstalk evaluation; however, it is necessary to be aware of its limitations:

1. Stimulation of a muscle motor point causes the activation of only a part of the muscle. It follows that crosstalk produced during stimulation is different from that produced during the maximal activation of the entire muscle. Furthermore, the myoelectric activity depends on the geometry and position of the signal source (the stimulated portion of the muscle), as well as on the phase relationships among MUAP due to the pool of active muscle fibers. As a consequence, it is not possible to sum crosstalk indices obtained during stimulation of different motor points of a muscle to obtain a more accurate estimation of the crosstalk index due to the whole muscle.
2. The crosstalk index, as defined in Reference 40, reflects volume conduction phenomena between the signal source and two different detection electrodes. By changing the position of the detection electrode above the stimulated muscle, the crosstalk index also changes, even if the volume conduction between the signal source and the detection electrode placed above the inactive muscle remains constant. It follows that standardization of the detection electrode position is necessary to be able to compare results obtained from different experiments.

C. Crosstalk among Leg and Thigh Muscles

DeLuca and Merletti[40] reported experiments carried out on 12 healthy subjects. They found an average crosstalk index of about 7% between tibialis anterior and peroneus brevis, while between tibialis anterior and soleus the crosstalk index was approximately 5%. No correlation was found between crosstalk index and leg circumference. Emley et al.[50] and Knaflitz et al.[86] found that, during supramaximal stimulation of the vastus medialis, signals up to 10.7% could be detected on the vastus lateralis, while smaller signals were detected on the rectus femoris and on the hamstrings. They also reported that stimulation of a motor point of the vastus lateralis generated crosstalk signals up to 18.2% on the rectus femoris and smaller signals were detected on the vastus medialis and the hamstrings.

XI. POSSIBLE APPLICATIONS IN DIAGNOSIS, SPORT, REHABILITATION, AND GERIATRIC MEDICINE

In diagnostic applications, electrical stimulation is used to evoke responses that in most cases are evaluated qualitatively and subjectively. In therapeutic and orthotic applications, much more attention is devoted to the mechanical rather than to the electrical muscle response. With few exceptions, despite the growing interest in electrotherapy, the information contained in the M-wave is not fully appreciated and applied at the clinical level.

In 1985, Cioni et al.[32] observed that 100% MVC and supramaximal stimulation of the peroneal nerve constitute two different ways of activating the tibialis anterior muscle. Motor unit activation is fully asynchronous in the first case and synchronous in the second. They found that the RMS of the surface myoelectric signal was not significantly different in the two legs of normal subjects with either paradigm. The ratio between the RMS of electrically evoked and voluntary signals measured at supramaximal stimulation and at 100% MVC, respectively, was found to be 3.22 ± 0.67 (mean $\pm$ standard deviation) in 40 normal muscles. In hemiparetic patients, the RMS of the electrically evoked response was neither significantly different in the two legs nor different from the normal value; however, the voluntary signal was significantly lower on the paretic side and the RMS ratio ranged from 5.1 to 9.3, providing a quantitative indication useful in assessing deficit and evaluating treatment. The technique was also used to assess gender-related differences.[33]

The analysis of electrically evoked myoelectric signals has the potential for quantification of training effects and for noninvasive characterization of muscle performance and resistance to fatigue.[71] Its applications in sport medicine are therefore obvious, but still very far from being fully investigated. Electrical stimulation is extensively and effectively applied in sport medicine either as a training technique or as a means to prevent disuse atrophy during immobilization consequent to bone fracture or ligament lesion (see References 35, 37, 91, 92, 98, and 145, among many others). The technique would be particularly useful in elderly individuals in whom the same pathologies have much more serious consequences than in younger subjects. A similar problem is encountered during long permanence in a microgravity environment in which electrical stimulation could be used to prevent muscle and bone deterioration; preliminary results concerning this application are promising.[46] Monitoring of the electrically evoked myoelectric signal could provide indications about the optimal treatment modality and duration as well as information about the muscle changes induced (or prevented) by a given condition or treatment.

Under electrical stimulation, the muscles of paraplegic subjects undergo fatigue at a faster rate than in normal subjects producing voluntary contractions of similar strength. Stimulation rates of 20 to 30 Hz are widely used to obtain tetanic contractions. These rates are near the upper values of physiological neural firings for most large skeletal muscles and therefore cause rapid fatigue.

Graupe and Kohn[66] have recently suggested that some parameters of the electrically evoked myoelectric signal could be used to monitor contraction effectiveness, to predict loss of contractile capability prior to its occurrence, and (possibly) to change the stimulation parameters or strategy in order to optimize performance. These goals are interesting but difficult because the intermittent nature of the contraction does not allow an easy prediction of force loss on the basis of the myoelectric signal (see Section IX), and the detected M-waves may be affected by movement artifacts since the contractions are not isometric and extensive muscle movement takes place underneath the detection electrodes. Considerably more research is needed to assess to what degree the myoelectric signal may be used to predict contractile capability during intermittent nonisometric contractions.

Electrical stimulation techniques have been applied in the investigation and/or treatment of muscle diseases. Edwards et al.[48] have used it as an objective technique to study Duchenne muscular dystrophy. They monitored muscle strength and found that the variance of force output in electrically evoked contractions was similar to that obtained with voluntary contractions, thereby ruling out motivational changes in favor of physiological changes. They also found that dystrophic muscles are slower to relax and less fatigable (in terms of mechanical output) than normal muscles. However, like most other investigators, they did not record the electrically evoked myoelectric signal. We believe that measurements of electrically evoked myoelectric signal CV and spectral variables might provide information useful for diagnosing the pathology as well as the effectiveness of the treatment. Spectral variables and CV of voluntary myoelectric signals have been used to assess muscular dystrophy and other pathologies.[54,67,76,137] If the repeatability of electrically evoked signal variables can be improved by surface nerve stimulation, then the ability of electrically evoked signals to resolve small variations might improve the present level of diagnosis and assessment.

ACKNOWLEDGMENTS

We thank Dr. L. R. Lo Conte and Mr. W. Conley for their support and cooperation. This work was supported by the U.S. Rehabilitation Research and Development Service of Veteran Affairs, by the Italian Ministry for University and Research, and by the Italian National Research Council within the framework of a collaboration agreement between the NeuroMuscular Research Center of Boston University and the Politecnico di Torino, Italy.

The authors are grateful to Dr. H. Broman of Chalmers University of Technology, Gothenburg, Sweden, for his review of this work and for many helpful suggestions.

APPENDIX: EFFECT OF SIGNAL TIME, SPACE, AND AMPLITUDE SCALING ON SPECTRAL, AMPLITUDE, AND AUTOCORRELATION FUNCTION VARIABLES

During a sustained contraction, the surface myoelectric signal may undergo amplitude scaling (by a factor h) due to reduction of the MUAPs amplitude, a frequency compression (by a factor k) due to reduction of muscle fiber CV or other factors, and a time delay d measured with respect to some time reference (e.g., a stimulation pulse).

These changes may be expressed mathematically through the following equations. Consider the real stationary signals $x_1(t)$ and $x_2(t) = hx_1(kt - d)$ with k, d, and h real and $0 < k < 1$. If $x_1(t)$ has Fourier transform $X_1(f)$, power spectral density $P_1(f) = |X_1(f)|^2$, and autocorrelation function $\Phi_{11}(\tau)$, the $x_2(t)$ has Fourier transform, power spectral density, and autocorrelation function given by:

$$X_2(f) = \frac{h}{k} X_1\left(\frac{f}{k}\right) e^{-j2\pi fd};$$

$$P_2(f) = \frac{h^2}{k^2} P\left(\frac{f}{k}\right);$$

$$\Phi_{22}(\tau) = \frac{h^2}{k} \Phi_{11}(k\tau) \tag{10}$$

The MNF of the power spectral density $P_1(f)$ is defined as:

$$f_{1mean} = \frac{\int_0^\infty f \cdot P_1(f)\, df}{\int_0^\infty P_1(f)\, df} \tag{11}$$

while the MDF of the power spectral density $P_1(f)$ is defined as:

$$\int_0^{f1med} P_1(f)\, df = \int_{f1med}^\infty P_1(f)\, df = \frac{1}{2}\int_0^\infty P_1(f)\, df \tag{12}$$

The lag of the first zero crossing of the autocorrelation function is defined as the lowest value τ_0 for which it is $\Phi_{11}(\tau_0) = 0$. The autocorrelation function is even and the width of its main lobe is $2\tau_0$.

The MNF and MDF of $P_2(f)$ are obtained by substituting $P_1(f)$ with $P_2(f)$ in the above equations. We define the MNF and MDF of $P_2(f)$ as f_{2mean} and f_{2med}. By further substituting $f/k = f'$ and $df = kdf'$ in the above equations, one obtains:

$$f_{2mean} = \frac{\int_0^\infty f \frac{h^2}{k^2} \cdot P_1\left(\frac{f}{k}\right) df}{\int_0^\infty \frac{h^2}{k^2} \cdot P_1\left(\frac{f}{k}\right) df} = \frac{k\int_0^\infty f' \cdot P(f')\, df'}{\int_0^\infty P(f')\, df'} = kf_{1mean} \tag{13}$$

and

$$\int_0^{kf_{med}} P_1(f')k\, df' = \int_{kf_{med}}^\infty P_1(f')k\, df' = \frac{1}{2}\int_0^\infty P_1(f')k\, df' \tag{14}$$

which implies

$$f_{2med} = kf_{1med} \tag{15}$$

Similarly, by substituting $kt = t'$ and $dt = dt'/k$ in the definition of autocorrelation, one obtains:

$$\Phi_{22}(\tau) = \frac{1}{k}\Phi_{11}(k\tau); \quad \tau_{02} = \frac{\tau_{01}}{k} \tag{16}$$

We define A_1 and R_1 as the ARV and the RMS values of $x_1(t)$ and A_2 and R_2 as the ARV and the RMS values of $x_2(t)$ over the time interval $0 - T$ (much greater than d) as:

$$A_1 = \frac{1}{T}\int_0^T |x_1(t)|\, dt;$$

$$R_1 = \sqrt{\frac{1}{T}\int_0^T x_1^2(t)\, dt} \tag{17}$$

$$A_2 = \frac{1}{T}\int_0^T |hx_1(kt + d)|\, dt;$$

$$R_2 = \sqrt{\frac{1}{T}\int_0^T h^2x_1^2(kt + d)\, dt} \tag{18}$$

by substituting $t' = kt$ and $dt = dt'/k$, by maintaining the same integration interval in the new time scale, and by assuming d negligible with respect to T we obtain:

$$A_2 = \frac{h}{kT}\int_0^T |x_1(t')|\,dt' = \frac{h}{k}A_1;$$
$$R_2 = \sqrt{\frac{h^2}{kT}\int_0^T x_1^2(t')\,dt'} = \frac{h}{\sqrt{k}}R_1 \quad (19)$$

If k changes slowly with time and may be assumed to be constant within an interval of duration T over which the power spectrum, the autocorrelation function, and the values A and R are estimated, then the signal may be assumed to be stationary over the interval of duration T. However, the signal will be nonstationary over subsequent intervals of duration T each, and all variables will be functions of time. The signals $x_1(t)$ and $x_2(t)$ may then be considered as two quasistationary epochs taken at times T_1 and T_2 of the same nonstationary signal. We may then define, for instance:

$$f_{1med} = f_{med}(0); \quad f_{2med} = f_{med}(t)$$
$$f_{1mean} = f_{mean}(0); \quad f_{2mean} = f_{mean}(t)$$
$$\tau_{01} = \tau_0(0); \quad \tau_{02} = \tau_0(t) \quad (20)$$

where t now indicates the epoch time and not the time within an epoch. It will then be

$$\frac{f_{med}(t)}{f_{med}(0)} = \frac{f_{mean}(t)}{f_{mean}(0)} = k;$$
$$\frac{\tau_0(t)}{\tau_0(0)} = \frac{1}{k}; \quad \frac{A(t)}{A(0)} = \frac{h}{k}; \quad \frac{R(t)}{R(0)} = \frac{h}{\sqrt{k}} \quad (21)$$

The above ratios are normalized values of the variables. In case of pure spectral compression (signal expansion in the time domain), with no change of spectral shape, it will then be

$$\frac{f_{med}(t)}{f_{med}(0)} = \frac{f_{mean}(t)}{f_{mean}(0)} = k;$$
$$\frac{f_{med}(t)}{f_{med}(0)}\frac{A(t)}{A(0)} = \frac{f_{mean}(t)}{f_{mean}(0)}\frac{A(t)}{A(0)} = h \quad (22)$$

$$\frac{f_{med}(t)}{f_{med}(0)}\frac{R(t)}{R(0)} = \frac{f_{mean}}{f_{mean}(0)}\frac{R(t)}{R(0)} = h\sqrt{k};$$

$$\frac{\tau_0(t)}{\tau_0(0)} = \frac{1}{k} \quad (23)$$

which implies:

$$\frac{f(t) - f(0)}{f(0)} = k - 1;$$
$$\frac{A(t) - A(0)}{A(0)} = \frac{h}{k} - 1 \quad (24)$$

$$\frac{f(t) - f(0)}{f(0)} = -k\frac{\tau_0(t) - \tau_0(0)}{\tau_0(0)} \quad (25)$$

where f stands for either f_{mean} or f_{med}.

Therefore, pure spectral compression implies equal percent changes in MNF and MDF. In such cases, the product of normalized MDF or MNF times normalized ARV is h and the percent change of either MNF or MDF is $-k$ times that of τ_0. If these conditions are verified, the PSD function is either compressing without changing shape or the shape changes are such as to satisfy the above set of conditions. The above conditions are necessary but not sufficient indicators of pure spectral compression as the only form of nonstationarity.

Frequency and amplitude scaling factors k and h may therefore be computed from normalized spectral and amplitude variables. In an ideal condition of spectral compression with no amplitude, scaling is $h = 1$. However, changes in MUAP amplitude and the addition or the removal of motor units from the active motor unit pool may lead to $h \neq 1$, as well as to changes of spectral shape, resulting in unequal percent changes in MNF and MDF during the contraction. The addition of new motor units would be likely to cause a faster increase in ARV and (possibly) a slower decrease in MDF and MNF, while de-recruitment of motor units would be likely to cause a slower increase or a decrease of ARV. If the motor units that drop out from the active pool are those contributing to the high frequency portion of the power density function (higher CV, relatively superficial units), MNF and MDF would be expected to decrease faster. These situations may be detected by observing the time course of the product of the normalized MNF (or MDF) time normalized ARV.

The concept and the consequences of spatial scaling may be understood by considering a source of electric field distributed (in space) along a segment of length L_f of a hypothetical fiber parallel to the skin. Such a source would generate a potential distribution (in space) of length L_s on the skin. We assume here that such potential distribution travels at a velocity v. Each spectral line of the frequency power spectrum (power density vs. frequency) of the signal detected by two electrodes on the skin would have a frequency $f = v/\lambda$, where λ is the corresponding line of the wavelength power spectrum (power density vs. wavelength). In particular, this equation would apply to the mean and median values of f and λ. If the potential distribution widens without changing shape, the wavelength power spectrum widens without changing shape and the frequency power spectrum compresses without changing shape. In other words, the frequency power spectrum is compressed by either an increase of L_s or a decrease of v, and either MNF or MDF are equally affected according to the equation $F(t) = C(v(t)/L_s(t))$, where C is a proportionality constant and $F(t)$ stands for either MDF or MNF as functions of time.

An increase of L_s would result from an increase of L_f, which, in this simple model, may be interpreted as the length of the depolarization zone of the hypothetical fiber. It is clear that, if such an increase takes place without any change of v, MNF and MDF would be affected but CV ($CV = v$) would be unchanged. A decrease in spectral variables would therefore take place without any change in CV. This fact would provide a possible explanation for the results shown in Figures 14 and 21.

REFERENCES

1. **Accornero, N., Bini, G., Lenzi, L. L., and Manfredi, M.,** Selective activation of peripheral nerve fibre groups of different diameter by triangular shaped stimulus pulses, *J. Physiol.*, 273, 539, 1977.
2. **Adrian, R. H. and Peachy, L. D.,** Reconstruction of the action potential of frog sartorius muscle, *J. Physiol.*, 235, 103, 1974.
3. **Alon, G., Allin, G., and Inbar, G.,** Optimization of pulse duration and pulse charge during transcutaneous electrical nerve stimulation, *Austr. J. Physiol.*, 29, 195, 1983.
4. **Alon, G.,** High voltage stimulation: effect of electrode size on basic excitatory responses, *Phys. Ther.*, 65, 890, 1985.
5. **Alpsan, D., Wormald, D.I., Lal, S., and Eccles, M. J.,** A system for selectively inactivating nerve fibres by a polarising transient current, *Med. Biol. Eng.*, 14, 90, 1976.
6. **Andreassen, S. and Ardent-Nielsen, L.,** Muscle fiber conduction velocity in motor units of the human anterior tibial muscle — a new size principle parameter, *J. Physiol.*, 391, 561, 1987.
7. **Arendt-Nielsen, L. and Mills, K. R.,** The relationship between mean power frequency of the EMG spectrum and muscle fiber conduction velocity, *EEG Clin. Neurophysiol.*, 60, 130, 1985.
8. **Arendt-Nielsen, L. and Zwarts, M.,** Measurement of muscle fiber conduction velocity in humans: techniques and applications, *J. Clin. Neurophysiol.*, 6, 173, 1989.
9. **Babb, T. L., Mariani, E., Strain, G. M., Lieb, J. P., Soper, H. V., and Crandall, P. H.,** A sample and hold amplifier system for stimulus artifact suppression, *EEG Clin. Neurophysiol.*, 44, 528, 1977.
10. **Badylak, S. F., Stevens, L., Janas, W., Gray, M. H., Geddes, L. A., and Voorhees, W. D., III,** Cardiac assistance with electrically stimulated skeletal muscle, *Med. Biol. Eng. Comput.*, 27, 159, 1989.
11. **Balestra, G., Knaflitz, M., and Merletti, R.,** Stationarity of voluntary and electrically elicited surface myoelectric signals, in *Electrophysiological Kinesiology*, Wallinga, W., Boom, H. B. K., and De Vries, J., Eds., Elsevier, Amsterdam, 261, 1988.
12. **Balestra, G., Knaflitz, M., and Merletti, R.,** Comparison between myoelectric signal mean and median frequency estimates, in *Proc. IEEE-EMBS 10th Annu. Int. Conf.*, New Orleans, 1988, 1708.
13. **Baratta, R., Ichie, M., Kwang, S. K., and Solomonow, M.,** Orderly stimulation of skeletal muscle motor units with tripolar nerve cuff, *IEEE Trans. BME*, 36, 836, 1989.
14. **Basmajian, J. and De Luca, C. J.,** *Muscles Alive*, 5th ed., Williams & Wilkins, Baltimore, 1985.
15. **Bellemare, F. and Bigland-Ritchie, B.,** Central components of diaphragmatic fatigue assessed by phrenic nerve stimulation, *J. Appl. Physiol.*, 62, 1307, 1987.
16. **Bergmans, J.,** Physiological observations on human single nerve fibers, in *New Developments in Electromyography and Clinical Neurophysiology*, Vol. 2, Desmedt, J. E., Ed., S. Karger, Basel, 1973, 89.
17. **Bigland-Ritchie, B.,** EMG and fatigue of human voluntary and stimulated contractions, in *Human Muscle Fatigue: Physiological Mechanisms*, Ciba

Foundation Symposium, Pitman Medical, London, 1981, 130.

18. **Bigland-Ritchie, B., Jones, D. A., and Woods, J. J.,** Excitation frequency and muscle fatigue: electrical responses during human voluntary and stimulated contractions, *Exp. Neurol.*, 64, 414, 1979.
19. **Blogg, T. and Reid, W. D.,** A digital technique for stimulus artifact reduction, *EEG Clin. Neurophysiol.*, 76, 557, 1990.
20. **Bonato, P., Balestra, G., Knaflitz, M., and Merletti, R.,** Comparison between muscle fiber conduction velocity estimation techniques: spectral matching vs. cross-correlation, in *Proc. 8th Int. Cong. ISEK*, Baltimore, 1990, 19.
21. **Bowman, B. R. and Baker, L. L.,** Effects of waveform parameters on comfort during transcutaneous neuromuscular electrical stimulation, *Ann. Biomed. Eng.*, 13, 59, 1985.
22. **Bowman, H. and McNeal, D.,** Response of single alpha motoneurons to high frequency pulse trains: firing behavior and conduction block phenomenon, *Appl. Neurophys.*, 49, 121, 1986.
23. **Brennen, A.,** The characterization of transcutaneous stimulating electrodes, *IEEE Trans. BME*, 23, 479, 1976.
24. **Brody, L., Pollock, M., Roy, S., De Luca, C., and Celli, B.,** pH induced effects on median frequency and conduction velocity of the myoelectric signal, *J. Appl. Physiol.*, 71, 1878, 1991.
25. **Broman, H., Bilotto, G., and De Luca, C. J.,** A note on the non-invasive estimation of muscle fiber conduction velocity, *IEEE Trans. BME*, 32, 341, 1985.
26. **Broman, H., Bilotto, G., and De Luca, C. J.,** Myoelectric signal conduction velocity and spectral parameters: influence of force and time, *J. Appl. Physiol.*, 8, 1428, 1985.
27. **Brown, W. F., Kadrie, H., and Milner-Brown, H.,** Rank order of recruitment of motor units with graded electrical stimulation of median of ulnar nerves in normal subjects and in patients with entrapment neuropathies, in *Motor Unit Types, Recruitment and Plasticity in Health and Disease*, Desmedt, J. E., Ed., S. Karger, Basel, 1981, 321.
28. **Buchthal, F., Guld, C., and Rosenfalck, P.,** Propagation velocity in electrically activated muscle fibers in man, *Acta Physiol. Scand.*, 34, 75, 1955.
29. **Buchthal, F., Guld, C., and Rosenfalck, P.,** Innervation zone and propagation velocity in human muscle, *Acta Physiol. Scand.*, 35, 174, 1955.
30. **Butikofer, R. and Lawrence, P. D.,** Electrocutaneous nerve stimulation. II. Stimulus waveform selection, *IEEE Trans. BME*, 26, 69, 1979.
31. **Cooper, R. G., Edwards, R. H. T., Gibson, H., and Stokes, M. J.,** Human muscle fatigue: frequency dependence of excitation and force generation, *J. Physiol.*, 397, 585, 1988.
32. **Cioni, R., Giannini, F., Paradiso, C., Battistini, N., Denoth, F., Navona, C., and Starita, A.,** Differences between surface EMG in male and female subjects evidenced by automatic analysis, *EEG Clin. Neurophysiol.*, 70, 306, 1988.
33. **Cioni, R., Paradiso, C., Battistini, N., Starita, A., Navona, C., and Denoth, F.,** Automatic analysis of surface EMG (preliminary findings in healthy subjects and in patients with neurogenic motor diseases), *EEG Clin. Neurophysiol.*, 61, 243, 1985.
34. **Crago, P. E., Peckham, P. J., Mortimer, T. J., and Van der Meulen, J.,** The choice of pulse duration for chronic electrical stimulation via surface, nerve and intramuscular electrodes, *Ann. Biomed. Eng.*, 2, 252, 1974.
35. **Currier, D. and Mann, R.,** Muscular strength development by electrical stimulation in healthy individuals, *Phys. Ther.*, 63, 915, 1983.
36. **Davies, S. W. and Parker, P. A.,** Estimation of myoelectric conduction velocity distribution, *IEEE Trans. BME*, 34, 365, 1987.
37. **Delitto, A., Rose, S., and McKowen, J.,** Electrical stimulation versus voluntary exercise in strengthening thigh musculature after ACL surgery, *Phys. Ther.*, 68, 660, 1988.
38. **Del Pozo, F. and Delgado, J. M. R.,** Hybrid stimulator for chronic experiments, *IEEE Trans. BME*, 25, 92, 1978.
39. **De Luca, C. J.,** Myoelectric manifestations of localized muscular fatigue in humans, *Crit. Rev. Biomed. Eng.*, 11, 251, 1984.
40. **De Luca, C. and Merletti, R.,** Surface myoelectric signal cross-talk among muscles of the leg, *EEG Clin. Neurophysiol.*, 69, 568, 1988.
41. **Denny-Brown, D.,** Interpretation of the electromyogram, *Arch. Neurol. Psychiatr.*, 61, 99, 1949.
42. **Dimitrov, G.,** Changes in the extracellular potentials produced by unmyelinated nerve fibers resulting from alterations in the propagation velocity or the duration of the action potential, *Electromyogr. Clin. Neurophysiol.*, 27, 243, 1987.
43. **Dimitrova, N.,** Influence of the length of depolarization in the extracellular potential field of a single unmyelinated nerve fibre, *Electromyogr. Clin. Neurophysiol.*, 13, 547, 1973.
44. **Duchateau, J. and Hainaut, K.,** Electrical and mechanical failures during sustained and intermittent contractions in humans, *J. Appl. Physiol.*, 58, 942, 1985.
45. **Duchateau, J., de Montigny, L., and Hainaut, K.,** Electro-mechanical failures and lactate production during fatigue, *Eur. J. Appl. Physiol.*, 56, 287, 1987.
46. **Duvoisin, M., Convertino, V., Buchanan, P., Gollink, P., and Dudley, G.,** Characteristics and preliminary observations of the influence of electromyostimulation on the size and function of human skeletal muscle during 30 days of simulated microgravity, *Aviat. Space Environ. Med.*, 60, 671, 1989.
47. **Edelberg, R.,** Electrical properties of the skin, in *Methods in Psychobiology*, Brown, C. C., Ed., Williams & Wilkins, Baltimore, 1967.

48. **Edwards, R., Chapman, S., Newman, D., and Jones, D.,** Practical analysis of variability of muscle function measurements in Duchenne muscular dystrophy, *Muscle Nerve,* 10, 6, 1987.
49. **Elden, H. R.,** *Biophysical Properties of the Skin,* Vol. 1, John Wiley & Sons, New York, 1971.
50. **Emley, M., Catani, F., Roy, S., and Knaflitz, M.,** Myoelectric crosstalk in antagonist muscles of the human thigh, *Proc. IEEE-EMBS 9th Annu. Int. Conf.,* Boston, 1987.
51. **Etnyre, B. and Abraham, L. D.,** Comparison of wire and surface electrode recordings between antagonist pairs of muscles, *Proc. 6th ISEK Congr.,* Tokyo, 1985.
52. **Fang, Z. and Mortimer, T.,** Selective activation of small motor axons by quasitrapezoidal current pulses, *IEEE Trans. BME,* 38, 168, 1991.
53. **Fang, Z. and Mortimer, T.,** A method to effect physiological recruitment order in electrically activated muscles, *IEEE Trans. BME,* 38, 175, 1991.
54. **Frascarelli, M., Rocchi, L., and Feaola, I.,** EMG computerized analysis of localized fatigue in Duchenne muscular dystrophy, *Muscle Nerve,* 11, 757, 1988.
55. **Freeman, J. A.,** An electronic stimulus artifact suppressor, *EEG Clin. Neurophysiol.,* 31, 170, 1971.
56. **Gans, B. and Kraft, G. H.,** M-response quantification: a technique, *Arch. Phys. Med. Rehab.,* 62, 376, 1981.
57. **Garland, S. J., Garner, S. H., and McComas, A. J.,** Relationship between numbers and frequencies of stimuli in human muscle fatigue, *J. Appl. Physiol.,* 65, 89, 1988.
58. **Garner, S. H., Hicks, A. L., and McComas, A. J.,** Prolongation of twitch potentiating mechanism throughout muscle fatigue and recovery, *Exp. Neurol.,* 103, 277, 1989.
59. **Gath, L. and Stalberg, E.,** On the volume conduction in human skeletal muscles: *in situ* measurements, *EEG Clin. Neurophysiol.,* 43, 106, 1977.
60. **Gatzke, R. D.,** The electrode: a measurement systems viewpoint, in *Biomedical Electrode Technology,* Miller, H. A. and Harrison, D. C., Eds., Academic Press, New York, 1974.
61. **Geddes, L. A.,** *Electrodes and the Measurement of Bioelectric Events,* Wiley-Interscience, New York, 1972.
62. **Gorman, P. H. and Mortimer, J. T.,** The effect of stimulus parameters on the recruitment characteristics of direct nerve stimulation, *IEEE Trans. BME,* 30, 407, 1983.
63. **Gorman, P. H., Mortimer, J. T., and Van den Honert, C.,** Enhancing excitability differences between nerve fibers, *Proc. 33rd ACEMB,* p. 63, 1980.
64. **Gottlieb, G. L., Myklebust, B. M., Penn, R. D., and Agarwal, G. C.,** Reciprocal excitation of muscle antagonists by the primary efferent pathway, *Exp. Brain Res.,* 46, 454, 1982.
65. **Gracanin, F. and Trnkoczy, A.,** Optimal stimulus parameters for minimum pain in the chronic stimulation of innervated muscle, *Arch. Phys. Med. Rehab.,* 56, 243, 1975.
66. **Graupe, D. and Kohn, K. H.,** A critical review of EMG-controlled electrical stimulation in paraplegics, *Crit. Rev. Biomed. Eng.,* 15, 187, 1988.
67. **Gruener, R., Stern, L., and Weisz, R.,** Conduction velocities in single fibers of diseased human muscle, *Neurology,* 29, 1293, 1979.
68. **Gydikov, A. and Kosarov, D.,** Influence of various factors on the length of the summated depolarized area of the muscle fibers in voluntary activating of motor units and in electrical stimulations, *Electromyogr. Clin. Neurophysiol.,* 14, 79, 1974.
69. **Gydikov, A., Gerilowsky, L., Gatev, P., and Kostev, K.,** Volume conduction of motor unit potentials from different human muscles to long distances, *Electromyography,* 22, 105, 1982.
70. **Gydikov, A., Kostov, K., Kossev, A., and Kosarov, D.,** Estimations of the spreading velocity and of parameters of the muscle potentials by averaging of the summated electromyogram, *Electromogr. Clin. Neurophysiol.,* 24, 191, 1984.
71. **Hainaut, K. and Duchateau, J.,** Muscle fatigue, effects of training and disuse, *Muscle Nerve,* 12, 660, 1989.
72. **Hakansson, C. H.,** Conduction velocity and amplitude of the action potential as related to circumference in the isolated fiber of frog muscle, *Acta Physiol. Scand.,* 37, 14, 1956.
73. **Hanson, J.,** The effects of repetitive stimulation on the action potential and the twitch of rat muscle, *Acta Physiol. Scand.,* 90, 387, 1974.
74. **Hary, D., Belman, M. J., Propst, J., and Lewis, S.,** A statistical analysis of the spectral moments used in the EMG test of endurance, *J. Appl. Physiol.,* 53, 779, 1982.
75. **Henriksson-Larsen, K., Friden, J., and Whetling, M.,** Distribution of fiber sizes in human skeletal muscle. An enzyme histochemical study in muscle tibialis anterior, *Acta Physiol. Scand.,* 123, 171, 1985.
76. **Hilfiker, P. and Meyer, M.,** Normal and myopatic propagation of surface motor unit action potentials, *EEG Clin. Neurophysiol.,* 57, 21, 1984.
77. **Hultman, E. and Sjoholm, H.,** Electromyogram, force and relaxation time during and after continuous electrical stimulation of human skeletal muscle *in situ, J. Physiol.,* 339, 33, 1983.
78. **Hunter, I. W., Kearney, R. E., and Jones, L. A.,** Estimation of the conduction velocity of muscle action potentials using phase and impulse response function techniques, *Med. Biol. Eng. Comput.,* 25, 121, 1987.
79. **Hutton, R. S., Roy, R. R., and Edgerton, R.,** Coexistent Hoffmann reflexes in human leg muscles are commonly due to volume conduction, *Exp. Neurol.,* 100, 265, 1988.

80. **Jones, D. A.,** Muscle fatigue due to changes beyond the neuromuscular junction, in *Human Muscle Fatigue: Physiological Mechanisms,* Ciba Foundation Symposium, Pitman Medical, London, 1982, 178.
81. **Jones, D. A., Bigland-Ritchie, B., and Edwards, R. T. H.,** Excitation frequency and muscle fatigue: mechanical responses during voluntary and stimulated contractions, *Exp. Neurol.,* 64, 401, 1979.
82. **Knaflitz, M. and Merletti, R.,** Suppression of stimulation artifacts from myoelectric evoked potential recordings, *IEEE Trans. BME,* 35, 758, 1988.
83. **Knaflitz, M.,** Sviluppo di Strumentazione, Metodologie e Algoritmi per l'Analisi ed il Controllo Non Invasivo del Sistema Neuromuscolare (in Italian), Ph.D. dissertation, Poltecnico di Torino, Torino, Italy, 1989.
84. **Knaflitz, M., Balestra, G., and Merletti, R.,** Relationship between SMES PSD and ACF main lobe width in localized muscle fatigue evaluation, in *Proc. 11th IEEE Annu. Int. Conf. Engineering in Medicine and Biology,* Seattle, Part 3, 11, 1024, 1989.
85. **Knaflitz, M., Merletti, R., and De Luca, C. J.,** Inference of motor unit recruitment order in voluntary and electrically elicited contractions, *J. Appl. Physiol.,* 68, 1657, 1990.
86. **Knaflitz, M., Merletti, R., and Catani, F.,** Crosstalk assessment in human thigh muscles, in *Electrophysiological Kinesiology,* Wallinga, W., Boom, H. B. K., and de Vries, J., Eds., Elsevier, Amsterdam, 1988, 261.
87. **Kostov, K., Kossev, A., and Gydikov, A.,** Utilization of the stimulated electromyogram for estimation of the functional state of the muscles, *Electromyogr. Clin. Neurophys.,* 24, 387, 1984.
88. **Kralj, A. and Bajd, T.,** *Functional Electrical Stimulation: Standing and Walking After Spinal Cord Injury,* CRC Press, Boca Raton, FL, 1989.
89. **Kranz, H., Williams, A. M., Cassell, J., Caddy, D. J., and Silberstein, R. B.,** Factors determining the frequency content of the electromyogram, *J. Appl. Physiol. Respir. Environ. Exercise Physiol.,* 55, 392, 1983.
90. **Krjnevic, K. and Miledy, R.,** Failure of neuromuscular propagation in rats, *J. Physiol.,* 140, 440, 1958.
91. **Lagasse, P., Boucher, J., Samson, J., and Jacques, L.,** Training effects of functional electrical stimulation in weightlifting, *J. Human Mov. Stud.,* 5, 61, 1979.
92. **Lainey, C., Walmsley, R., and Andrew, G.,** Effectiveness of exercise alone versus exercise plus electrical stimulation in strengthening the quadriceps muscle, *Physiol. Can.,* 35, 5, 1983.
93. **Lam, H. S., Morgan, D. L., and Lampard, D. G.,** Derivation of reliable electromyograms and their relation to tension in mammalian skeletal muscles during synchronous stimulation, *EEG Clin. Neurophysiol.,* 46, 72, 1979.
94. **Lateva, Z.,** Dependence of quantitative parameters of the extracellular potential power spectrum on propagation velocity, duration and asymmetry of action potentials, *Electromyogr. Clin. Neurophysiol.,* 28, 191, 1988.
95. **Lawrence, J. H. and De Luca, C. J.,** Myoelectric signal versus force relationship in different human muscles, *J. Appl. Physiol.,* 54, 1653, 1983.
96. **Lewis, D. M.,** The physiology of motor units in mammalian skeletal muscle, in *Handbook of Behavioral Neurobiology,* Vol. 5, Towe and Luschei, Eds., Plenum Press, New York, 1981.
97. **Lindstrom, L. and Magnusson, R.,** Interpretation of myoelectric power spectra: a model and its applications, *Proc. IEEE,* 65, 653, 1977.
98. **Lloyd, T., De Domenico, G., Strauss, G., and Singer, K.,** A review of the use of electromotor stimulation in human muscles, *Austr. J. Physiol.,* 32, 18, 1986.
99. **Malek, A. M. and Mark, R. G.,** Functional electrical stimulation of the latissimus dorsi muscle for use in cardiac assist, *IEEE Trans. BME,* 36, 781, 1989.
100. **Mangun, G. R., Mulkey, R. M., Young, B., and Goslow, G. E.,** 'Cross-talk' in EMG, *Electromyography,* 26, 443, 1986.
101. **Marsden, C. D., Meadows, J. C., and Merton, P. A.,** Fatigue in human muscle in relation to the number and frequency of motor impulses, *Proc. Physiol. Soc.,* p. 94P, 1976.
102. **Mason, J. L. and McKay, N. A. M.,** Pain sensation associated with electrocutaneous stimulation, *IEEE Trans. BME,* 23, 405, 1976.
103. **Masuda, T., Miyano, H., and Sadoyama, T.,** The measurement of muscle fiber conduction velocity using gradient threshold zero crossing method, *Med. Biol. Eng. Comput.,* 29, 673, 1982.
104. **McComas, A., Fawcet, J., Campbell, M., and Sica, R.,** Electrophysiological estimation of the number of motor units within a human muscle, *J. Neurol. Neurosurg. Psychiatr.,* 34, 121, 1971.
105. **McComas, A., Sica, R., and Campbell, M.,** Numbers and sizes of human motor units in health and disease, in *New Developments in Electromyography and Clinical NeuroPhysiology,* Desmedt, J., Ed., Vol. 1, S. Karger, Basel, 1973, 55.
106. **McComas, A.,** Motor units estimation: methods, results, and present status, *Muscle Nerve,* 14, 585, 1991.
107. **McNeal, D. and Baker, L.,** Effect of joint angle, electrodes and waveform on electrical stimulation of the quadriceps and hamstrings, *Ann. Biomed. Eng.,* 16, 299, 1988.
108. **McGill, K., Cummings, K. L., Dorfman, L. J., Berlizot, B. B., Leutkemeyer, K., Nishimura, D. G., and Widrow, B.,** On the nature and elimination of stimulus artifact in nerve signals, *Evol. Med. Biol. Eng.,* Seville, Spain, 1986.
109. **McGill, K. and Dorfman, L.,** High resolution alignment of sampled waveforms, *IEEE Trans. BME,* 31, 462, 1984.

110. **Merletti, R., Sabbahi, M., and De Luca, C.,** Median frequency of the myoelectric signal: effects of muscle ischemia and cooling, *Eur. J. Appl. Physiol.*, 52, 258, 1984.

111. **Merletti, R. and De Luca, C. J.,** New techniques in surface electromyography, in *Computer Aided Electromyography and Expert Systems*, Desmedt, J. E., Ed., Elsevier, Amsterdam, 1989, chap. 9.

112. **Merletti, R., Knaflitz, M., and De Luca, C. J.,** Myoelectric manifestations of fatigue in voluntary and electrically elicited contractions, *J. Appl. Physiol.*, 69, 1810, 1990.

113. **Merletti, R., Lo Conte, L. R., and Orizio, C.,** Indices of muscle fatigue, *J. Electromyogr. Kinesiol.*, 1, 20, 1991.

114. **Merletti, R., Lo Conte, L. R., Cisari, C., and Actis, M. V.,** Age related changes in surface myoelectric signals, *Scand. J. Rehab. Med.*, in press.

115. **Merletti, R., Balestra, G., and Knaflitz, M.,** Effect of FFT based algorithms on estimation of myoelectric signal apectral parameters, *Proc. 11th IEEE Annu. Int. Conf. Engineering in Medicine and Biology*, Seattle, Part 3, 11, 1022, 1989.

116. **Merletti, R. and De Luca, C. J.,** Crosstalk in surface electromyography, in *Computer Aided Electromyography and Expert Systems*, Desmedt, J.E., Ed., Elsevier, Amsterdam, 1989, chap. 11.

117. **Merton, P. A., Hill, D. K., and Morton, H. B.,** Indirect and direct stimulation of fatigued human muscle, in *Human Muscle Fatigue: Physiological Mechanisms*, Ciba Foundation Symposium, Pitman Medical, London, 1981, 120.

118. **Miller, R. N. and Rinzel, J.,** The dependence of impulse propagation speed on firing frequency dispersion, for the Hodgkin-Huxley model, *Biophys. J.*, 34, 227, 1981.

119. **Mills, K. R.,** Power spectral analysis of EMG and compound muscle action potential during muscle fatigue and recovery, *J. Physiol.*, 326, 401, 1982.

120. **Milner, M. and Quambury, A.,** Force, pain and electrode size in the electrical stimulation of leg muscles, *Nature*, 223, 645, 1969.

121. **Milner-Brown, H. S. and Miller, R. G.,** Muscle membrane excitation and impulse propagation velocity are reduced during muscle fatigue, *Muscle Nerve*, 9, 367, 1986.

122. **Mizrahi, J., Susak, Z., Isakov, E., Solzi, P., and Najenson, T.,** Optimization of stimulus parameters for reduced fatiguability during standing by functional electrical stimulation of paraplegics, Proc. 4th Mediterranean Conf. Medicine and Biology in Engineering, Seville, Spain, 1986.

123. **Morimoto, S. and Masuda, T.,** Dependence of conduction velocity on spike interval during voluntary muscular contraction in human motor units, *Eur. J. Appl. Physiol.*, 53, 195, 1984.

124. **Moritani, T., Muro, M., and Kijima, A.,** Electromechanical changes during electrically induced and voluntary contractions: electrophysiologic responses of different muscle fibre types during stimulated contractions, *Exp. Neurol.*, 88, 471, 1985.

125. **Moritani, T., Muro, M., Kijima, A., Gaffney, F. A., and Parsons, D.,** Electromechanical changes during electrically induced and voluntary contractions: surface and intramuscular EMG responses during sustained and maximal voluntary contraction, *Exp. Neurol.*, 88, 484, 1985.

126. **Morrenhof, J. W. and Abbink, H. J.,** Crosscorrelation and crosstalk in surface EMG, *Electromyography*, 25, 73, 1985.

127. **Mortimer, J. T.,** Motor prosthesis, in *Handbook of Physiology*, Section 1, *The Nervous System*, Vol. 2, Motor Control, Part 1, 1984, 155. Published by the American Physiol. Society, distributed by Williams and Wilkins.

128. **Myklebust, B., Gottlieb, G. L., Agarwal, G. C., and Penn, R. D.,** Reciprocal excitation of antagonist muscles as a differentiating feature in spasticity, *Ann. Neurol.*, 12, 367, 1982.

129. **Naeije, M. and Zorn, H.,** Estimation of action potential conduction velocity in human skeletal muscles using the surface EMG cross-correlation technique, *Electromyogr. Clin. Neurophysiol.*, 23, 73, 1983.

130. **Nelson, H., Smith, M., Bowman, B., and Waters, R.,** Electrode effectiveness during transcutaneous motor stimulation, *Arch. Phys. Med. and Rehab.*, 61, 73, 1980.

131. **Nielsen, R. P., Hayward, L. F., and Hutton, R. S.,** Concomitant (reciprocal excitation) short latency EMG reflexes in triceps surae and tibialis anterior muscles: volume conduction as a confounding variable, *Soc. Neurosci. Abstr.*, 12, 682, 1986.

132. **Oppenheim, A. W. and Shafer, R. W.,** *Digital Signal Processing*, Prentice-Hall, Englewood Cliffs, NJ, 1975.

133. **Papoulis, A.,** *Probability, Random Variables, and Stochastic Processes*, McGraw-Hill, New York, 1984.

134. **Plonsey, R.,** *Bioelectric Phenomena*, McGraw-Hill, New York, 1969.

135. **Parker, M., Berthold, M., Brown, R., Hunter, S., Smith, M., and Runhling, R.,** Fatigue response in human quadriceps femoris muscle during high frequency electrical stimulation, *J. Orthopaed. Sports Phys. Ther.*, 7, 145, 1986.

136. **Perry, J., Esterday, C. S., and Antonelli, D. J.,** Surface versus intramuscular electrodes for electromyography of superficial and deep muscles, *Phys. Ther.*, 1, 7, 1981.

137. **Preising, B., Hull, M., Taylor, R., and Shumway, R.,** Carrier detection of Duchenne dystrophy by frequency analysis of the electromyogram, *J. Biomed. Eng.*, 10, 417, 1988.

138. **Rau, G., Schnider, J., and Silny, J.,** The influence of temperature and excitation pattern on non-invasively detected conduction velocity in single motor units, *Proc. 10th IEEE Eng. Med. Biol. Soc. Annu. Int. Conf.*, p. 1702, 1988.

139. **Reucher, H., Rau, G., and Silny, J.,** Spatial filtering of non-invasive multielectrode EMG. I. Introduction to measuring techniques and applications, *IEEE Trans. BME*, 34, 98, 1987.

140. **Reucher, H., Rau, G., and Silny, J.,** Spatial filtering of non-invasive multielectrode EMG. II. Filter performance in theory and modeling, *IEEE Trans. BME,* 34, 106, 1987.
141. **Roby, R. J. and Lettich, E.,** A simplified system for artifact suppression, *EEG Clin. Neurophysiol.,* 39, 85, 1975.
142. **Roskar, E. and Roskar, A.,** Microcomputer based electromyographic recording system with stimulus artifact suppression, in 3rd Mediterranean Conf. Biomedical Engineering, Sect. 1.6, Portoroz, Yugoslavia, 1983.
143. **Roy, S. H., De Luca, C. J., and Schneider, J.,** Effects of electrode location on myoelectric condution velocity and median frequency estimates, *J. Appl. Physiol.,* 61, 1510, 1986.
144. **Sandercock, T. G., Faulkner, J. A., Albers, J. W., and Albrecht, P. H.,** Single motor unit and fiber action potentials during fatigue, *J. Appl. Physiol.,* 58(4), 1073, 1985.
145. **Singer, K.,** The influence of unilateral electrical muscle stimulation on motor unit activity patterns in atrophic human quadriceps, *Austr. J. Physiol.,* 32, 31, 1986.
146. **Sollie, G., Hermens, H. J., Boon, K. L., Wallinga de Jonge, W., and Zilvold, G.,** The measurement of conduction velocity of muscle fibers with surface EMG according to the cross-correlation method, *Electromyogr. Clin. Neurophysiol.,* 25, 193, 1985.
147. **Solomonow, M., Baratta, R., Shoji, H., and D'Ambrosia, R. D.,** The myoelectric signal of electrically stimulated muscle during recruitment: an inherent feedback parameter for a closed loop control scheme, *IEEE Trans. BME,* 33, 735, 1986.
148. **Solomonow, M., Eldred, E., Lyman, J., and Foster, J.,** Fatigue considerations of muscle contractile force during high-frequency stimulation, *Am. J. Phys. Med.,* 62, 117, 1983.
149. **Solomonow, M., Baratta, R., Miwa, T., Shoji, H., and D'Ambrosia, R. D.,** A technique for recording the EMG of electrically stimulated skeletal muscle, *Orthopedics,* 8, 492, 1985.
150. **Solomonow, M., Baratta, R., Zhou, B. H., Shoji, H., and D'Amrosia, R. D.,** The EMG-force model of electrically stimulated muscle: dependence on control strategy and predominant fiber composition, *IEEE Trans. BME,* 34, 692, 1987.
151. **Solomonow, M., Baratta, R., Baten, C., Smit, J., Hermens, H., Shoji, H., and D'Ambrosia, R. D.,** Electromyogram power spectra frequencies associated with motor unit recruitment strategies, *J. Appl. Physiol.,* 68, 1177, 1990.
152. **Solomonow, M.,** External control of the neuromuscular system, *IEEE Trans. BME,* 31, 752, 1984.
153. **Spencer, H. J.,** An automatic, optically isolated, biphasic constant current stimulator adaptor for artifact suppression, *EEG Clin. Neurophysiol.,* 51, 215, 1981.
154. **Stephens, W. G. L.,** The current-voltage relationship in human skin, *Med. Electron. Biol. Eng.,* 1, 389, 1963.
155. **Stokes, M. J., Edwards, R. T. H., and Cooper, R. G.,** Effect of low frequency fatigue on human muscle strength and fatigability during subsequent stimulated activity, *Eur. J. Appl. Physiol.,* 59, 278, 1989.
156. **Stulen, F. and De Luca, C. J.,** Frequency parameters of the myoelectric signal as a measure of muscle conduction velocity, *IEEE Trans. BME,* 28, 512, 1981.
157. **Swanson, D. K. and Webster, J. G.,** A model for skin-electrode impedance, in *Biomedical Technology,* Miller, H. A. and Harrison, D. C., Eds., Academic Press, New York, 1974.
158. **Walker, D. D. and Kimura, J.,** A fast recovery electrode amplifier for electrophysiology, *EEG Clin. Neurophysiol.,* 45, 789, 1978.
159. **Wheeler, B. and Smith, S.,** High-resolution alignment of action potential waveforms using cubic spline interpolation, *J. Biomed. Eng.,* 9, 47, 1987.
160. **Zajac, F. E. and Faden, J. S.,** Relationship among recruitment order, axonal conduction velocity, and muscle-unit properties of type-identified motor units in cat plantaris muscle, *J. Neurophysiol.,* 53, 1303, 1985.
161. **Zhou, B. H., Baratta, R., and Solomonow, M.,** Manipulation of muscle force with various rate and recruitment control strategies, *IEEE Trans. BME,* 34, 128, 1987.
162. **Zijdewind, C., Bosch, W., Goessens, L., Kandou, T. W. A., and Kernell, D.,** Electromyogram and force during stimulated fatigue tests of muscles in dominant and non-dominant hands, *Eur. J. Physiol.,* 60, 127, 1990.
163. **Zorn, H. and Naeije, M.,** Online muscle fiber action potential conduction velocity measurements using the surface EMG cross-correlation technique, *Med. Biol. Eng. Comput.,* 21, 239, 1983.